Cell Biology
Developmental Biology

Wnt induces FZD5/8 endocytosis and degradation and the involvement of RSPO-ZNRF3/RNF43 and DVL

Reviewed Preprint
v2 • August 13, 2025
Revised by authors

Reviewed Preprint
v1 • January 20, 2025

Dong Luo, Jing Zheng, Shuning Lv, Ren Sheng, Maorong Chen, Xi He, Xinjun Zhang

Key Laboratory of Molecular Biophysics of the Ministry of Education, College of Life Science and Technology, Huazhong University of Science and Technology, Wuhan, China • The Sichuan Provincial Key Laboratory for Human Disease Gene Study and Department of Laboratory Medicine, Center for Medical Genetics, Sichuan Provincial People's Hospital, School of Medicine, University of Electronic Science and Technology of China, Chengdu, China • College of Life and Health Science, Northeastern University, Shenyang, China • Center for Life Sciences, School of Life Sciences, Yunnan University, Kunming, China • The F. M. Kirby Neurobiology Center, Boston Children's Hospital, Department of Neurology, Harvard Medical School, Boston, United States • Research Unit for Blindness Prevention of the Chinese Academy of Medical Sciences (2019RU026), Sichuan Academy of Medical Sciences and Sichuan Provincial People's Hospital, Chengdu, China

eLife Assessment

This study presents **important** findings demonstrating that the internalization and degradation of FZD5 and FZD8, two of the ten Frizzled proteins, are WNT dependent and do not involve DVL. The evidence supporting the claims of the authors is **convincing**. This research will be of interest to biologists specializing in Wnt signaling, cancer, and regenerative medicine.

https://doi.org/10.7554/eLife.103996.2.sa3

Abstract

Frizzled (FZD) proteins are the principal receptors of the Wnt signaling pathway. However, whether Wnt ligands induce FZD endocytosis and degradation remains elusive. The transmembrane E3 ubiquitin ligases ZNRF3 and RNF43 were reported to promote the endocytosis and degradation of FZD receptors to inhibit Wnt signaling, and their function is antagonized by R-spondin (RSPO) proteins. However, the dependency of RSPO-ZNRF3/RNF43-mediated FZD endocytosis and degradation on Wnt stimulation, as well as the specificity of this degradation for different FZD, remains unclear. Here, we demonstrated that Wnt induces FZD5/8 endocytosis and degradation in a ZNRF3/RNF43-dependent manner. ZNRF3/RNF43 selectively targets FZD5/8 for degradation upon Wnt stimulation. RSPO1 enhances Wnt signaling by specifically stabilizing FZD5/8. Wnt promotes the interaction between FZD5 and RNF43. We further demonstrated that DVL proteins promote ligand-independent endocytosis of FZD but are dispensable for Wnt-induced FZD5/8 endocytosis and degradation. Our results reveal a novel negative regulatory mechanism of Wnt signaling at the receptor level and

illuminate the mechanism by which RSPO-ZNRF3/RNF43 regulates Wnt signaling, which may provide new insights into regenerative medicine and cancer therapy.

Introduction

The evolutionarily conserved Wnt signaling pathways play pivotal roles in embryonic development and adult tissue homeostasis (Clevers and Nusse, 2012; Nusse and Clevers, 2017; Rim et al., 2022; Stapornwongkul and Vincent, 2021; Steinhart and Angers, 2018). There are nineteen Wnt ligands and ten Frizzled (FZD) receptors in mammals (Wang et al., 2016). Wnt-FZD complexes activate several intracellular signaling pathways, including the canonical (Wnt/β-catenin) and noncanonical pathways. In the Wnt/β-catenin pathway, certain Wnt-FZD complexes engage and phosphorylate the coreceptors LRP5/6, inhibiting β-catenin phosphorylation and degradation, and stabilized cytosolic β-catenin is translocated to the nucleus, where it activates the TCF/LEF1 transcription factors to induce target gene expression. The noncanonical pathways, mainly the Wnt/PCP and Wnt/Ca^{2+} pathways, are activated by Wnt-FZD complexes with the assistance of the coreceptors ROR1/2, VANGL, RYK, and/or PTK7. These pathways regulate cell and tissue polarity, movement and gene expression (Niehrs, 2012). Wnt signaling pathways are tightly regulated at different levels to maintain normal physiological functions (Jiang and Cong, 2016; Rim et al., 2022). Multiple Wnt pathway mutations have been identified as driver events in human cancers, and several therapeutic strategies have been developed (Anastas and Moon, 2013; Bugter et al., 2021; O'Brien et al., 2023).

Receptor endocytosis serves as a common regulatory mechanism across multiple signaling pathways. Numerous studies have reported that receptor endocytosis positively influences both the canonical and noncanonical Wnt pathways by facilitating or amplifying intracellular signaling (Chen et al., 2003; Yamamoto et al., 2006; Yu et al., 2007; Zhang et al., 2017). Conversely, ligand-induced receptor endocytosis and degradation play critical roles in controlling signal strength and duration and are typical negative regulatory mechanisms in receptor tyrosine kinase pathways (Alexander, 1998; Haglund and Dikic, 2012; Marmor and Yarden, 2004; Sorkin and Waters, 1993). However, whether Wnt induces FZD receptor endocytosis and degradation remains poorly characterized.

ZNRF3 and RNF43 are closely related transmembrane E3 ubiquitin ligases that are induced by Wnt/β-catenin signaling and antagonize Wnt signaling by promoting FZD receptor endocytosis and degradation (Bugter et al., 2024; Hao et al., 2012; Koo et al., 2012). However, how ZNRF3/RNF43 recognize FZD receptors is still controversial (Farnhammer et al., 2023; Hao et al., 2016; Tsukiyama et al., 2021). A recent report suggested that ZNRF3/RNF43 ubiquitinates FZD receptors through binding to DVL proteins, which were previously thought to regulate FZD protein endocytosis (Chen et al., 2003; Jiang et al., 2015). Another study proposed that ZNRF3/RNF43 interact with FZD receptors via their extracellular protease-associated (PA) domain (Tsukiyama et al., 2015). R-spondin (RSPO) family proteins of stem cell growth factors were reported to potentiate Wnt signaling by binding to and degrading ZNRF3/RNF43 with the help of LGR4 or LGR5 (Hao et al., 2012; Kazanskaya et al., 2004; Park et al., 2020; Xie et al., 2013). However, recent studies have indicated that RSPO can activate Wnt signaling through ZNRF3/RNF43 independently of LGRs (Dubey et al., 2020; Lebensohn and Rohatgi, 2018; Szenker-Ravi et al., 2018). Whether RSPO-ZNRF3/RNF43-mediated regulation of FZD receptors relies on Wnt stimulation and whether there are specificities toward different FZDs remain unclear.

In this study, we first demonstrated that Wnt induces FZD5/8 endocytosis and degradation in a ZNRF3/RNF43-dependent manner. We further demonstrated that DVL proteins promote ligand-independent FZD receptor endocytosis but do not affect Wnt-induced FZD5/8 endocytosis and degradation. Furthermore, we reevaluated the functions of ZNRF3/RNF43 and RSPO1 in regulating Wnt signaling. Our results suggest that RSPO1-ZNRF3/RNF43 specifically regulates FZD5/8 levels in

the presence of Wnt ligands. We also showed that Wnt induces the FZD5−RNF43 interaction at the plasma membrane. Our study reveals a novel mechanism for the regulation of Wnt signaling at the receptor level and provides further insights into the function of RSPO1-ZNRF3/RNF43 in the Wnt signaling pathways.

Results

Wnt induces FZD5/8 endocytosis and degradation

To investigate whether Wnt induces endocytosis and degradation of FZD receptors, HEK293A cells stably expressing each of the ten V5-FZDs (with the V5 tag added to the amino terminus of each FZD after the signal peptide) were treated with control, Wnt3a-conditioned or Wnt5a-conditioned medium (CM), and the FZD levels on the cell surface were examined via flow cytometry with an anti-V5 antibody. Both Wnt3a and Wnt5a dramatically reduced the expression of FZD5 and FZD8 on the cell surface without significantly affecting other FZD receptors (**Figure 1A**). Immunoblotting revealed that both Wnt3a and Wnt5a reduced the mature protein levels of both FZD5 and FZD8 (the upper bands of FZD5 and FZD8) (**Figure 1B**) (Chen et al., 2020; Koo et al., 2012). Treatment with the lysosomal inhibitor bafilomycin A1 rescued the mature form of FZD5 that was reduced by Wnt3a and Wnt5a (**Figure 1C**), suggesting that Wnt induced FZD5 degradation through the lysosomal pathway. We further showed that these phenomena are not specific to 293A cells, as Wnt3a and Wnt5a also induced FZD5/8 endocytosis and degradation in both Huh7 and U2OS cells (**Figure 1-figure supplement 1A-D**). These results suggest that Wnt3a and Wnt5a specifically promote the endocytosis and lysosomal degradation of FZD5/8.

FZD receptors are classified into four clusters, with sequence variations predominantly in the extracellular CRD domain and C-terminal tail (Huang and Klein, 2004). To investigate which domain is required for Wnt-induced FZD5 endocytosis, we generated FZD5 constructs with deletion of the CRD domain (△CRD) or C-terminal tail (△C) and analyzed them via flow cytometry. The results indicated that the CRD domain, but not the C-terminal tail, is crucial for Wnt3a/Wnt5a-induced FZD5 endocytosis (**Figure 1D-F**). Additionally, we constructed chimeric FZD proteins with swapped CRD domains, as illustrated in the schematic diagram (**Figure 1G**). For example, FZD4CRD-FZD5 consists of the CRD domain of FZD4 and FZD5 lacking the CRD domain. Wnt3a or Wnt5a treatment reduced the cell surface levels of FZD5CRD-FZD4 and FZD5CRD-FZD7 but had little effect on the cell surface levels of FZD4CRD-FZD5 or FZD7CRD-FZD5 (**Figure 1H**). These results suggest that Wnt-induced FZD5/8-specific endocytosis relies on their CRD domains.

As the commercially available anti-FZD antibodies either cannot detect endogenous proteins or can only recognize the immature form (data not shown), to visualize endogenous FZD5, we generated an FZD5 knock-in HEK293A cell line in which a V5 tag was inserted into the carboxyl terminus of the FZD5 locus before the stop codon via the CRISPR/Cas9 system and homologous recombination. Like V5-FZD5 overexpression, the endogenous FZD5-V5 protein exhibited two major bands on immunoblotting, and both the Wnt3a and Wnt5a treatments reduced the intensity of the upper band representing the mature form of FZD5, which occurred as early as one hour after treatment (**Figure 2A**). Using the same approach, we generated a FZD7-V5 knock-in cell line and observed that neither Wnt3a nor Wnt5a induced degradation of endogenous FZD7 (**Figure 2B**). Furthermore, treatment with the Porcupine inhibitor IWP-2 increased the level of the endogenous mature FZD5 protein but did not affect FZD7 levels (**Figure 2C**). Flow cytometry with anti-FZD5/8 or anti-FZD4 monoclonal antibodies revealed that IWP-2 treatment increased the cell surface levels of FZD5/8 but had little effect on FZD4 levels in HEK293A cells (**Figure 2D** and **E**) (Pan et al., 2021; Sachdev Sidhu, 2021; Steinhart et al., 2017). IWP-2 treatment also increased the cell surface levels of FZD5/8 in Huh7, MCF7 and 769P cells (**Figure 2-figure**

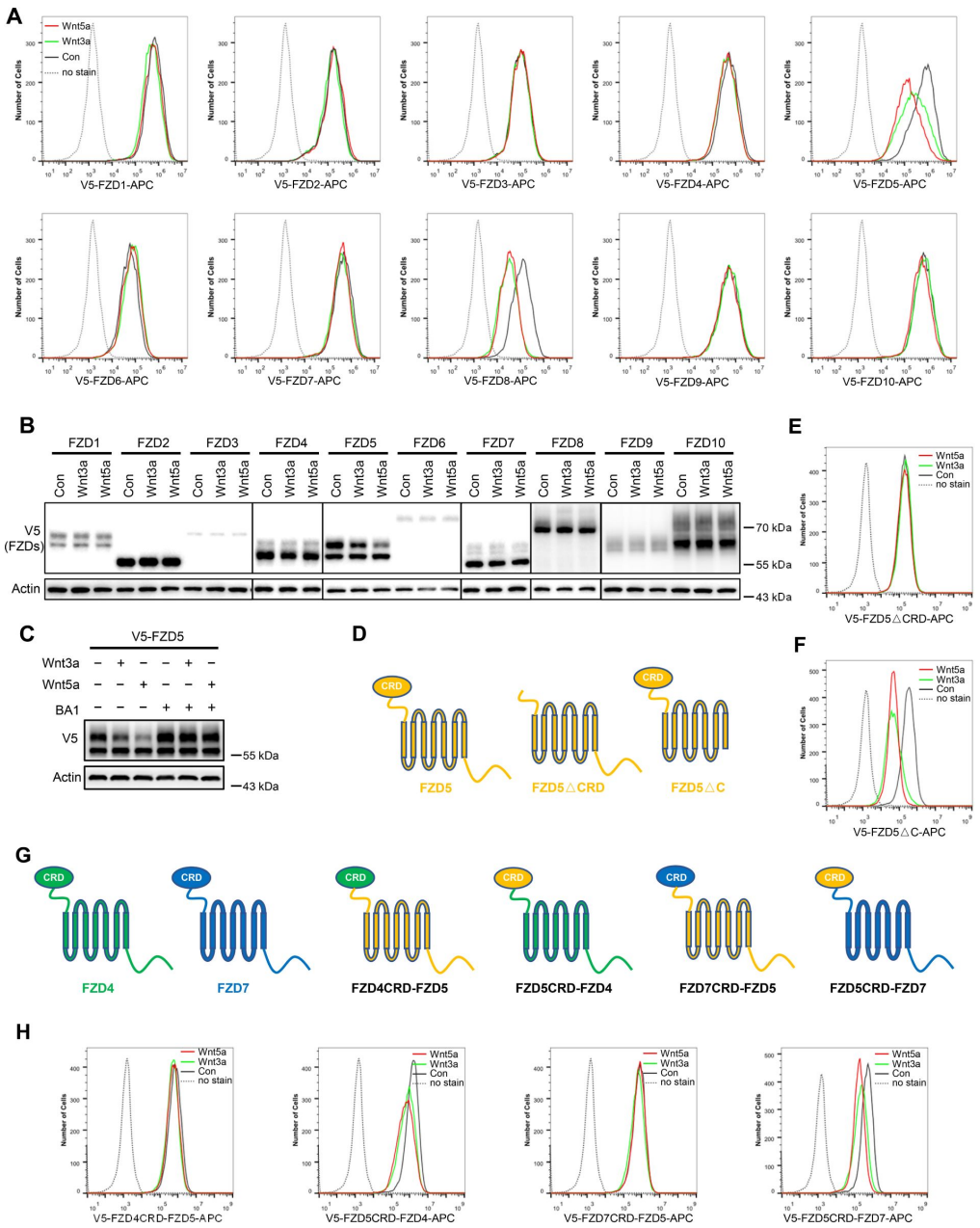

Figure 1.

Wnt induces FZD5/8 endocytosis and degradation.

(A) Wnt3a or Wnt5a specifically reduced the cell surface levels of V5-FZD5/8. HEK293A cells stably expressing each of the 10 V5-FZDs (FZD1 to 10) were treated with control, Wnt3a, or Wnt5a CM for 4 hours, and the cell surface levels of V5-FZDs were analyzed via flow cytometry using an anti-V5 antibody.
(B) Wnt3a or Wnt5a specifically decreased the levels of mature forms of V5-FZD5/8. The whole-cell lysates (WCLs) from the indicated cells treated as described in (A) were analyzed by immunoblotting with the indicated antibodies.
(C) Bafilomycin A1 (BA1) restored Wnt3a- or Wnt5a-induced FZD5 degradation.
(D) Schematic diagram of FZD5 constructs: full-length FZD5, FZD5 lacking the extracellular cysteine-rich domain (FZD5△CRD), and FZD5 lacking the intracellular C-terminus (FZD5△C). (E, F) HEK293A cells stably expressing the FZD5 truncation constructs shown in (D) were treated and analyzed as described in (A).
(G) Schematic diagram of CRD-swapped chimeric FZDs.
(H) HEK293A cells stably expressing the indicated chimeric FZD constructs shown in (F) were treated and analyzed as described in (A).

supplement 1A-C). The specificity of the anti-FZD5/8 and anti-FZD4 antibodies was confirmed in HEK293A cells overexpressing all ten FZD receptors (**Figure 2-figure supplement 2**). These results further indicate that Wnt induces the endocytosis and degradation of endogenous FZD5/8.

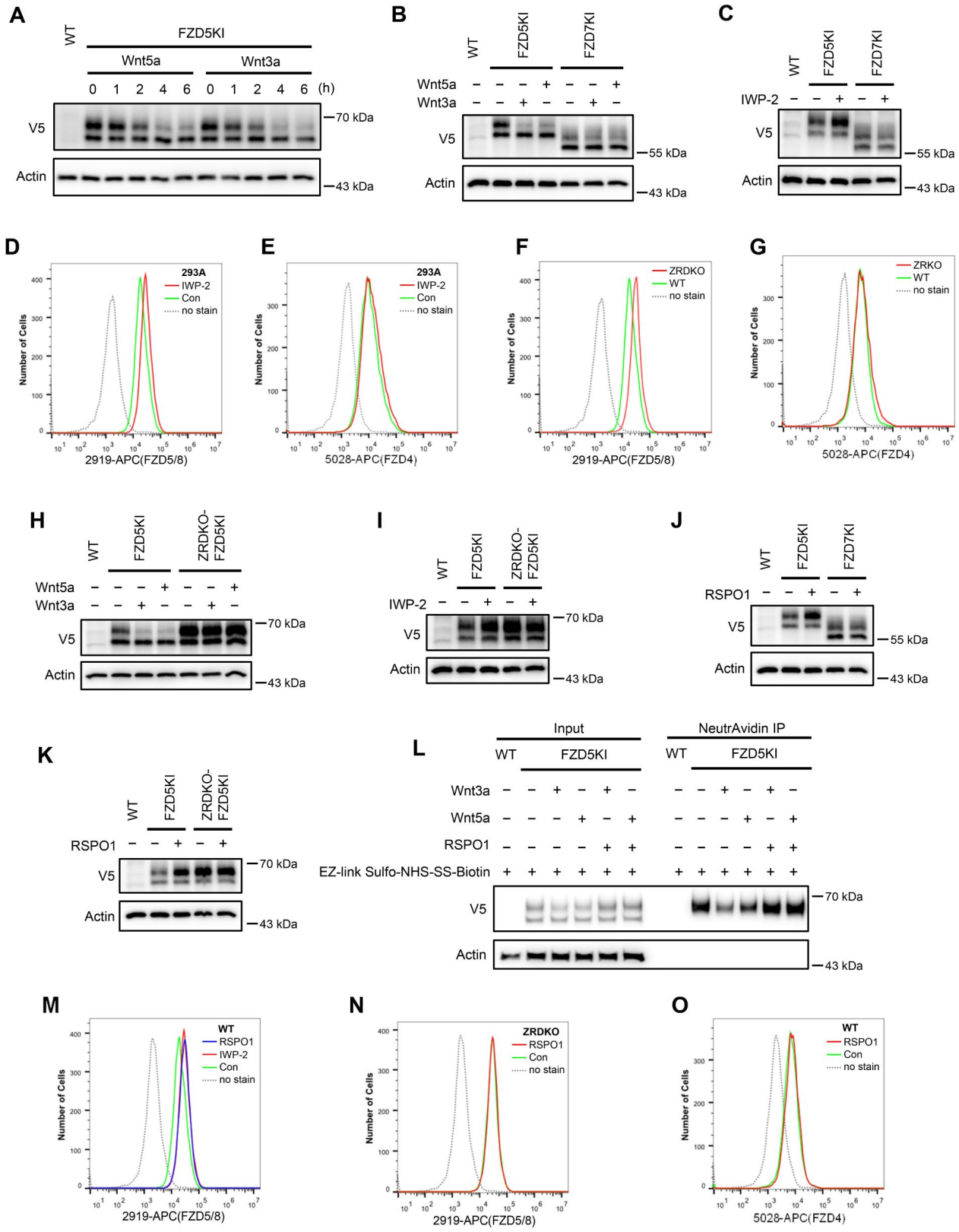

Figure 2.

Wnt induces ZNRF3/RNF43-dependent FZD5/8 endocytosis and degradation.

(A) Wnt3a or Wnt5a induced the degradation of endogenous FZD5. HEK293A cells with a V5 epitope tag knocked in at the C-terminus of endogenous FZD5 (FZD5KI) were treated with Wnt3a or Wnt5a CM for the indicated durations, and the WCLs were analyzed by immunoblotting with the indicated antibodies. Wild-type (WT) cells served as a negative control to confirm the specificity of the FZD5KI bands. The upper bands represent mature FZD5, whereas the lower bands represent immature FZD5.

(B) Wnt3a or Wnt5a induced the degradation of endogenous FZD5 but not FZD7. FZD5KI or FZD7KI (generated as described for FZD5KI) HEK293A cells were treated with control, Wnt3a CM or Wnt5a CM for 2 hours, and the WCLs were subjected to immunoblotting with the indicated antibodies.

(C) The Porcupine inhibitor IWP-2 increased the level of the endogenous mature form of FZD5 but not FZD7. FZD5KI or FZD7KI cells were treated overnight with or without IWP-2 (2.5 μM), and the WCLs were subjected to immunoblotting with the indicated antibodies.

(D, E) IWP-2 increased the cell surface levels of endogenous FZD5/8 but not FZD4. HEK293A WT cells were treated with or without IWP-2 and analyzed by flow cytometry to determine the FZD5/8 and FZD4 levels on the cell surface with anti-FZD5/8 (2919) or anti-FZD4 (5028) monoclonal antibodies. APC, allophycocyanin.

(F, G) *ZNRF3/RNF43* double knockout increased the cell surface levels of endogenous FZD5/8 but not FZD4. The cell surface levels of FZD5/8 and FZD4 in WT or ZRDKO cells were analyzed by flow cytometry.

(H) Wnt-induced FZD5 degradation is dependent on endogenous ZNRF3 and RNF43. WT, FZD5KI, or ZRDKO-FZD5KI (*ZNRF3/RNF43* double knockout cells with a V5 tag knocked in at the C-terminus of endogenous FZD5) cells were treated and analyzed as described in (B).

(I) IWP-2 did not increase the endogenous FZD5 protein level in ZRDKO cells.

(J) RSPO1 treatment increased the level of the mature form of endogenous FZD5 but not FZD7. FZD5KI and FZD7KI cells were treated with control or RSPO1 CM for 4 hours, and the WCLs were analyzed by immunoblotting with the indicated antibodies.

(K) RSPO1 failed to increase the level of the mature form of FZD5 in ZRDKO cells. FZD5KI or ZRDKO-FZD5KI cells were treated and tested as described in (J).

(L) Wnt3a and Wnt5a induced degradation of cell surface FZD5, which was restored by RSPO1. HEK293A FZD5KI cells were incubated with EZ-linked Sulfo-NHS-SS-Biotin to label cell surface proteins and then treated with control, Wnt3a, Wnt5a CM or Wnt3a/Wnt5a with RSPO1 CM. The labeled proteins were precipitated by NeutrAvidin beads and eluted for immunoblotting.

(M) IWP-2 and RSPO1 treatments similarly increased the FZD5/8 levels on the cell surface. WT cells were treated with IWP-2 overnight or RSPO1 for 4 hours, followed by flow cytometry analysis.

(N, O) RSPO1 treatment did not increase the cell surface levels of FZD5/8 in ZRDKO cells or FZD4 in WT cells. HEK293A ZRDKO or WT cells were treated with control or RSPO1 CM for 4 hours and subjected to flow cytometry analysis with anti-FZD5/8 or anti-FZD4 monoclonal antibodies.

Wnt-induced FZD5/8 degradation relies on ZNRF3/RNF43

ZNRF3 and RNF43 are homologous transmembrane E3 ubiquitin ligases that have been reported to target FZD receptors for endocytosis and degradation (Farnhammer et al., 2023; Hao et al., 2012; Koo et al., 2012). We wondered whether Wnt-induced FZD5/8 endocytosis and degradation depend on ZNRF3/RNF43. To address this, we generated a *ZNRF3/RNF43* double-knockout HEK293A cell line (ZRDKO) via the CRISPR/Cas9 technique, which was verified by sequencing (**Figure 2-Figure Supplement 3**). Flow cytometry analysis with the anti-FZD5/8 antibody revealed that *ZNRF3/RNF43* double knockout increased FZD5/8 levels on the cell surface (**Figure 2F**), which is consistent with previous reports (Hao et al., 2012; Koo et al., 2012). In contrast, the membrane levels of FZD4 remained unchanged in ZRDKO cells (**Figure 2G**). We subsequently established an FZD5-V5 knock-in cell line based on ZRDKO. Immunoblotting revealed that neither Wnt3a nor Wnt5a induced the degradation of endogenous mature FZD5 in ZRDKO cells (**Figure 2H**). Additionally, IWP-2 treatment did not further increase mature FZD5 levels in ZRDKO cells (**Figure 2I**).

RSPO proteins antagonize ZNRF3/RNF43, thereby potentiating Wnt signaling (Hao et al., 2012; Xie et al., 2013; Yan et al., 2017). Given that ZNRF3/RNF43 specifically degrades FZD5/8 in the presence of Wnt, we examined whether RSPO1 treatment could specifically increase FZD5/8 levels. Immunoblotting revealed that RSPO1 significantly increased the level of endogenous mature FZD5 but did not affect the FZD7 level (**Figure 2J**). Moreover, RSPO1 had little effect on FZD5 levels in ZRDKO cells (**Figure 2K**). Furthermore, a cell surface biotinylation assay revealed that Wnt3a or Wnt5a induced degradation of cell surface FZD5, which was antagonized by cotreatment with RSPO1 (**Figure 2L**). Flow cytometry analysis of wild-type (WT) HEK293A cells treated with IWP-2 or RSPO1 revealed that both treatments similarly elevated FZD5/8 levels on the cell surface (**Figure 2M**). However, RSPO1 treatment did not increase membrane FZD5/8 levels in ZRDKO cells or FZD4 levels in WT cells (**Figure 2N-O**).

Taken together, these results suggest that ZNRF3/RNF43 degrades FZD5/8 under Wnt stimulation, which is antagonized by RSPO.

DVL proteins regulate Wnt-independent FZD endocytosis and are dispensable for Wnt-induced FZD5/8 endocytosis or degradation

DVL proteins have been reported to regulate FZD endocytosis and degradation by binding to ZNRF3/RNF43 and recruiting it to FZD receptors (Jiang et al., 2015; Yu et al., 2007). We investigated whether DVL proteins are required for Wnt-induced FZD5/8 endocytosis and degradation. To address this, we generated a *DVL1/2/3* triple-knockout HEK293A cell line (DVLTKO), which was verified by genomic sequencing and immunoblotting (**Figure 3A**, **Figure 3-Figure Supplement 1**). Flow cytometry analysis revealed that triple knockout of *DVL1/2/3* increased the cell surface levels of FZD5/8 (**Figure 3B**), suggesting that DVL proteins promote FZD5/8 endocytosis, which is consistent with a previous report (Jiang et al., 2015). However, both IWP-2 and RSPO1 treatments further elevated the cell surface levels of FZD5/8 in DVLTKO cells (**Figure 3C** and **D**), indicating that Wnt may still induce ZNRF3/RNF43-dependent FZD5/8 endocytosis even in the absence of DVL proteins. Furthermore, Wnt3a and Wnt5a reduced both the cell surface level and the mature form of the FZD5 protein in DVLTKO cells stably expressing V5-FZD5, as assessed by flow cytometry and immunoblotting (**Figure 3E** and **F**).

To visualize FZD endocytosis dynamics, we performed an antibody-labeled endocytosis assay. WT, DVLTKO and DVLTKO cells re-expressing DVL2 (DVLTKO+DVL2) stably expressing V5-linker-FZD5 were first treated with IWP-2 overnight to inhibit the secretion of endogenous Wnt proteins. The cells were labeled with an anti-V5 antibody and then treated with control, Wnt3a CM or Wnt5a CM for 1 hour (**Figure 3G**), and the internalized antibody was visualized by immunostaining. The

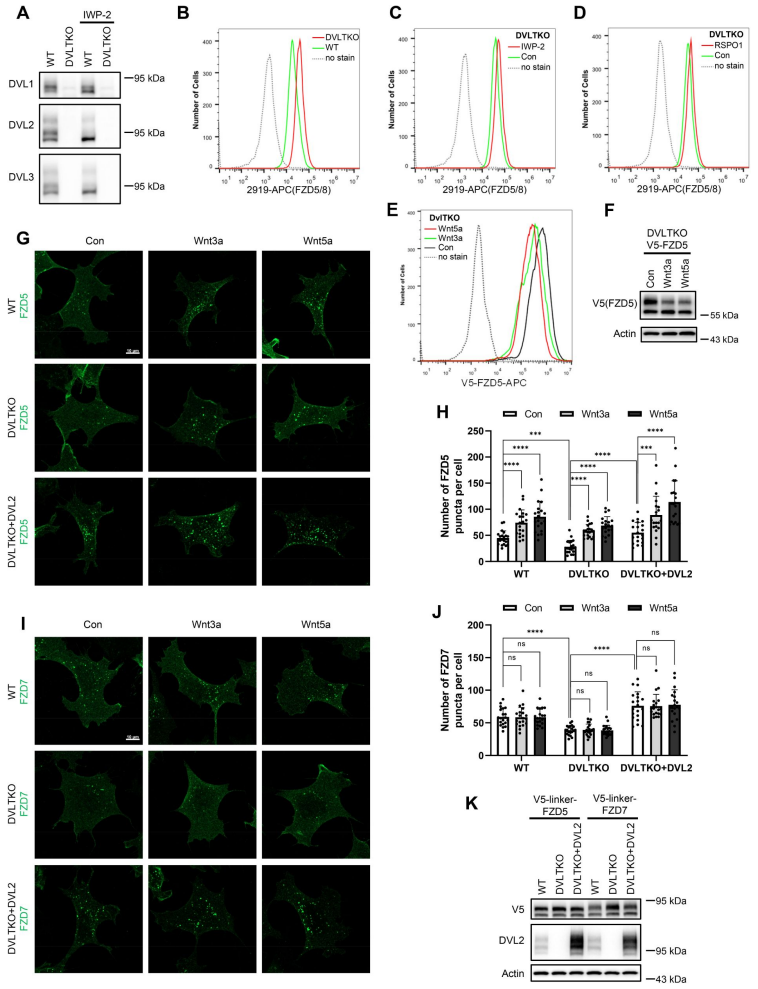

Figure 3.

DVL proteins participate in ligand-independent FZD protein endocytosis but are not required for Wnt-induced FZD5/8 endocytosis or degradation.

(A) Validation of HEK293A DVLTKO cells by immunoblotting analysis with the indicated anti-DVL antibodies.
(B) Triple knockout of *DVL1/2/3* increased FZD5/8 levels on the cell surface. WT and DVLTKO cells were analyzed by flow cytometry with an anti-FZD5/8 monoclonal antibody.
(C, D) IWP-2 (C) or RSPO1 (D) treatment increased FZD5/8 levels on the cell surface of DVLTKO cells. DVLTKO cells were treated with IWP-2 overnight or RSPO1 for 4 hours, followed by flow cytometry analysis.
(E) Wnt3a or Wnt5a treatment reduced the cell surface levels of V5-FZD5 in DVLTKO cells. HEK293A DVLTKO cells stably expressing V5-FZD5 were treated with control, Wnt3a CM or Wnt5a CM for 4 hours and analyzed via flow cytometry with an anti-V5 antibody.
(F) Wnt3a or Wnt5a treatment decreased the mature form of V5-FZD5 in DVLTKO cells. The cells in (E) were treated, and the WCLs were analyzed by immunoblotting with the indicated antibodies.
(G, I) Triple knockout of *DVL1/2/3* reduced ligand-independent FZD5 and FZD7 endocytosis but had no effect on Wnt3a- or Wnt5a-induced FZD5 endocytosis. Indicated HEK293A cells stably expressing V5-linker-FZD5 or V5-linker-FZD7 were first incubated with an anti-V5 antibody, and the cells were treated with control, Wnt3a or Wnt5a CM for 1 hour and subjected to immunofluorescence analysis. The cells were treated with IWP-2 overnight prior to treatment with conditioned medium. Scale bars, 10 μm.
(H, J) Quantification of the number of FZD5 (G) or FZD7 (I) puncta in WT, DVLTKO and DVLTKO + DVL2 cells (mean ± SD, n = 20 cells per group). ns, no significant difference; ***p < 0.001; ****p < 0.0001.
(K) WCLs from WT, DVLTKO and DVLTKO + DVL2 cells stably expressing V5-linker-FZD5 or V5-linker-FZD7 were analyzed by immunoblotting.

linker sequence was used to separate the V5 tag from the FZD5 protein to avoid interference with Wnt5a binding. Compared with WT cells, DVLTKO cells presented fewer FZD5 puncta in the control CM-treated group, and re-expressing DVL2 in DVLTKO cells elevated FZD5 puncta, whereas Wnt3a and Wnt5a increased the number of FZD5 puncta in both WT, DVLTKO and DVLTKO+DVL2 cells, as quantified by the number of FZD5 puncta (**Figure 3H**). Compared with WT cells, DVLTKO cells presented decreased FZD7 internalization in control CM, which could also be rescued by re-expressing DVL2, and Wnt3a or Wnt5a CM had no effect on FZD7 endocytosis in WT, DVLTKO or DVLTKO+DVL2 cells (**Figure 3I-J**). Whole-cell lysates from WT, DVLTKO and DVLTKO+DVL2 cells expressing V5-linker-FZD5 or V5-linker-FZD7 were analyzed by immunoblotting to verify the expression of FZDs and DVL2 (**Figure 3K**).

Collectively, these results suggest that DVL proteins participate in Wnt-independent FZD receptor endocytosis but are dispensable for Wnt-induced FZD5/8 endocytosis and degradation.

ZNRF3/RNF43 promotes the degradation of internalized FZD5 but is dispensable for Wnt-induced FZD5 internalization

We next investigated the role of ZNRF3/RNF43 in the process of Wnt-induced FZD5/8 endocytosis and degradation. We found that Wnt3a or Wnt5a CM treatment reduced the cell surface level of V5-FZD5 in ZRDKO cells, as determined by flow cytometry (**Figure 4A**), although they had little effect on the total protein level of FZD5 (**Figure 4B**), suggesting that Wnt induces FZD5 internalization independent of ZNRF3/RNF43. We further performed an immunostaining assay to visualize the cellular trafficking route of internalized FZD5 after Wnt3a and Wnt5a treatment for various durations. The results revealed that a significant amount of FZD5 was internalized into the intracellular vesicles in both WT and ZRDKO cells after Wnt3a or Wnt5a treatment for one hour, and the FZD5 signals gradually diminished in WT but not ZRDKO cells after Wnt treatment for two and four hours (**Figure 4C**, **Figure 4-Figure supplement 1A**), indicating that ZNRF3/RNF43 is required for the degradation of internalized FZD5 but not for Wnt-induced FZD5 internalization. Furthermore, cotreatment with RSPO1 prevented FZD5 degradation but had little effect on FZD5 internalization induced by Wnt3a or Wnt5a (**Figure 4D**, **Figure 4-figure supplement 1B**). Under Wnt treatment, internalized FZD5 colocalized with either EEA1, an early endosomal marker, or LAMP1, a lysosomal marker, in WT cells, whereas this colocalization was significantly reduced in ZRDKO cells (**Figure 4E-H**). These results suggest that ZNRF3/RNF43 promotes endolysosomal transport and degradation of internalized FZD5, whereas in ZRDKO cells, internalized FZD5 may be recycled back to the plasma membrane for reuse.

Reevaluation of the function of ZNRF3/RNF43 in Wnt signaling

Previous studies have suggested that ZNRF3/RNF43 degrades FZD receptors independently of Wnt ligands (Farnhammer et al., 2023; Jiang et al., 2015; Tsukiyama et al., 2015). However, our finding that Wnt induces ZNRF3/RNF43-dependent FZD5/8 degradation indicates that the functions of ZNRF3/RNF43 in FZD endocytosis and degradation are modulated by Wnt ligands. These results prompted us to reevaluate the function of ZNRF3/RNF43 in Wnt signaling. Although HEK293A cells stably expressing V5-FZD5 or V5-FZD7 presented significantly higher FZD protein levels on the cell surface than ZRDKO cells did, as measured by flow cytometry with an anti-pan-FZD antibody (**Figure 5A**), these cells presented markedly lower cytosolic β-catenin levels than ZRDKO cells did (**Figure 5B**). The increase in DVL protein phosphorylation and cytosolic β-catenin observed in *ZNRF3/RNF43* double knockout cells could be reversed by IWP-2 treatment, whereas IWP-2 had a minimal effect on DVL phosphorylation in cells overexpressing V5-FZD5 or V5-FZD7 (**Figure 5C** and **D**). These findings suggest that elevated Wnt signaling in ZRDKO cells cannot be solely attributed to increased FZD protein levels on the cell surface.

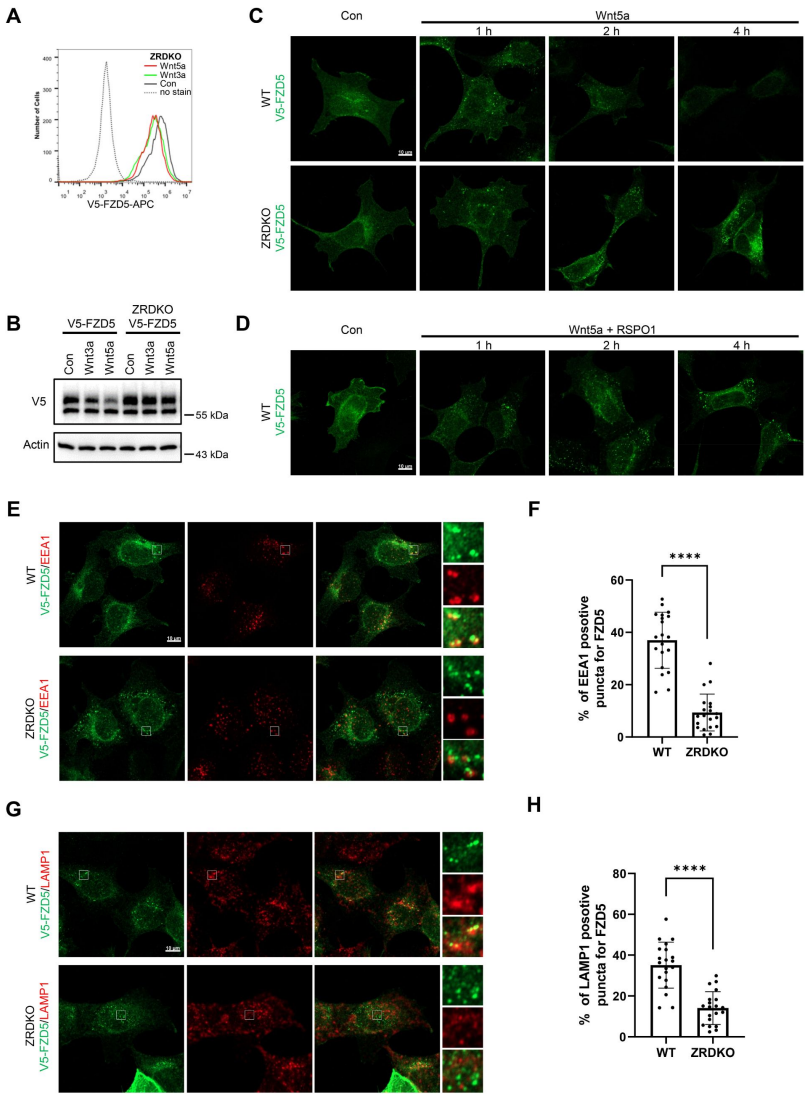

Figure 4.

ZNRF3/RNF43 is required for the degradation of internalized FZD5 but is dispensable for Wnt-induced FZD5 internalization.

(A) Wnt3a and Wnt5a induced V5-FZD5 endocytosis in ZRDKO cells.
(B) Wnt3a and Wnt5a induced V5-FZD5 degradation in WT but not ZRDKO cells.
(C) Wnt5a induced FZD5 internalization in both WT and ZRDKO cells, and internalized FZD5 gradually diminished in WT but not ZRDKO cells. WT or ZRDKO cells stably expressing V5-FZD5 were treated with control or Wnt5a CM for the indicated times and analyzed by immunostaining. The cells were treated with IWP-2 overnight prior to treatment with CM. Scale bars, 10 μm.
(D) Cotreatment with RSPO1 prevented FZD5 degradation but had little effect on FZD5 internalization induced by Wnt5a. The cells were treated with IWP-2 overnight prior to treatment with CM. Scale bars, 10 μm.
(E) Compared with those in WT cells, fewer V5-FZD5 puncta colocalized with the early endosomal marker EEA1 in ZRDKO cells. WT or ZRDKO cells stably expressing V5-FZD5 were treated with control or Wnt5a CM for 2 hours and then analyzed by immunostaining. The cells were treated with IWP-2 overnight prior to treatment with CM. Scale bars, 10 μm.
(F) Quantification of the percentage of V5-FZD5 puncta colocalized with EEA1 in WT and ZRDKO cells (mean ± SD, n = 20 cells per group). ****$p < 0.0001$.
(G) Compared with those in WT cells, fewer V5-FZD5 puncta colocalized with the lysosomal marker LAMP1 in ZRDKO cells. WT or ZRDKO cells stably expressing V5-FZD5 were treated with control or Wnt5a CM for 2 hours and then analyzed by immunostaining. The cells were treated with IWP-2 overnight prior to treatment with CM. Scale bars, 10 μm.
(H) Quantification of the percentage of V5-FZD5 puncta colocalized with LAMP1 in WT and ZRDKO cells (mean ± SD, n = 20 cells per group). ****$p < 0.0001$.

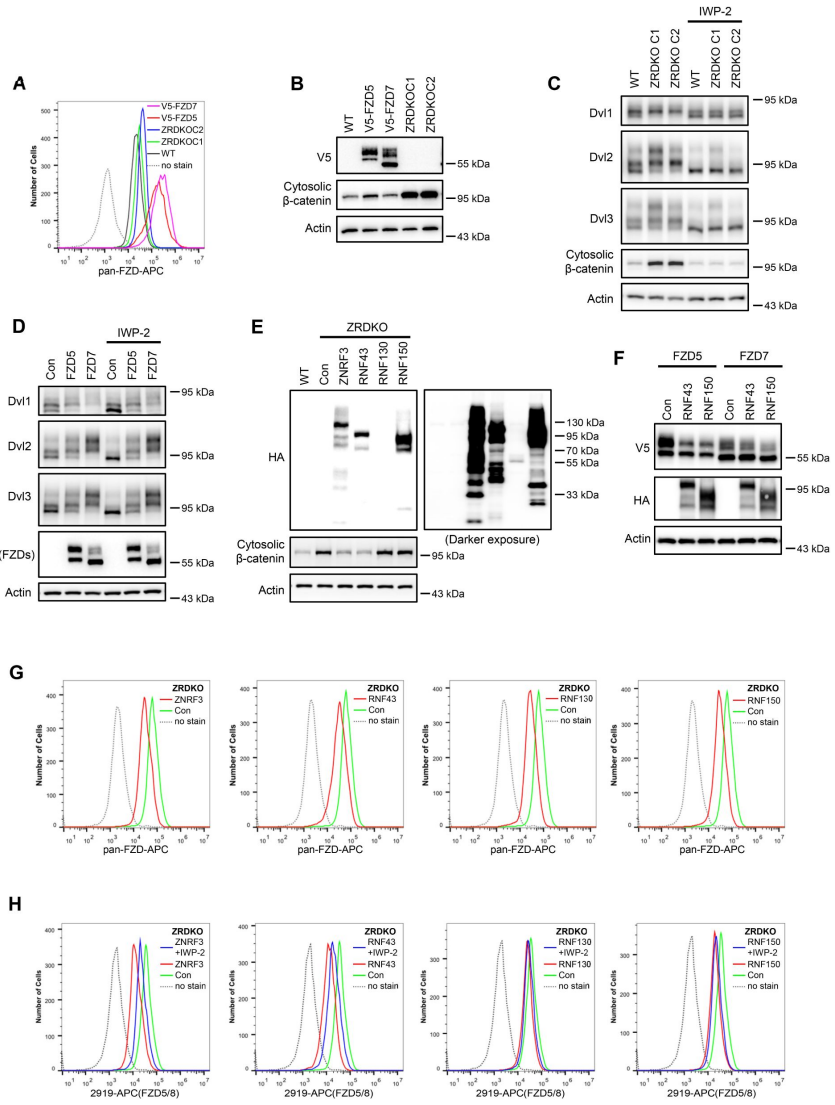

Figure 5.

ZNRF3/RNF43-mediated inhibition of Wnt signaling cannot be explained by simply regulating FZD levels on the cell surface.

(A) Flow cytometry analysis of FZD levels on the cell surface of WT HEK293A, ZRDKO (ZRDKO C1/2), and HEK293A cells stably expressing V5-FZD5/7 with an anti-pan-FZD monoclonal antibody. FZD levels on the cell surface were greater in ZRDKO cells than in WT cells but much lower than those in V5-FZD5/7-expressing cells.
(B) Cytosolic β-catenin levels were significantly lower in V5-FZD5/7-expressing cells than in ZRDKO cells.
(C) *ZNRF3/RNF43* double knockout-induced DVL phosphorylation and cytosolic β-catenin accumulation depend on endogenous Wnt proteins. WT or ZRDKO cells were treated with or without IWP-2 and analyzed by immunoblotting.
(D) Overexpressing V5-FZD5 or V5-FZD7 resulted in Wnt-independent DVL phosphorylation. V5-FZD5/7-expressing cells were treated with or without IWP-2, and the WCLs were analyzed by immunoblotting.
(E) Expression of ZNRF3 or RNF43, but not RNF130 or RNF150, reversed the increase in cytosolic β-catenin levels in ZRDKO cells.
(F) Overexpression of RNF43 or RNF150 reduced the levels of mature forms of V5-FZD5 or V5-FZD7. WCLs from HEK293A cells expressing V5-FZD5 or V5-FZD7 alone or together with RNF43-HA or RNF150-HA were analyzed by immunoblotting.
(G) Overexpression of ZNRF3, RNF43, RNF130, or RNF150 in ZRDKO cells reduced FZD levels on the cell surface, as measured by flow cytometry with an anti-pan-FZD antibody.
(H) Overexpression of ZNRF3, RNF43, RNF130, or RNF150 in ZRDKO cells reduced FZD5/8 levels on the cell surface. IWP-2 partially reversed the reduction in FZD5/8 levels induced by ZNRF3 or RNF43 but not by RNF130 or RNF150. The cells in (E) were treated with or without IWP-2 overnight and analyzed by flow cytometry with an anti-FZD5/8 monoclonal antibody.

Furthermore, reintroducing ZNRF3 or RNF43 into ZRDKO cells efficiently decreased the cytosolic β-catenin level, whereas the expression of RNF130 or RNF150, two structurally similar transmembrane E3 ubiquitin ligases, did not (**Fig. 5E**). However, expressing RNF43 or RNF150 in HEK293A cells stably expressing V5-FZD5 or V5-FZD7 efficiently decreased the levels of the mature forms of FZD5 and FZD7 (**Figure 5F**). Each of these E3 ligases reduced FZD protein levels on the cell surface of the ZRDKO cells to a comparable degree, as determined by flow cytometry with an anti-pan-FZD antibody (**Figure 5G**). Furthermore, each of the four E3 ligases also reduced FZD5/8 levels on the cell surface in ZRDKO cells, with IWP-2 partially restoring the effects of ZNRF3 and RNF43 but not those of RNF130 or RNF150 (**Figure 5H**). Taken together, these results suggest that overexpressing a transmembrane E3 ubiquitin ligase may nonspecifically degrade FZD receptors and that the specific ability of ZNRF3 and RNF43 to degrade FZD is dependent on Wnt ligands.

ZNRF3/RNF43 inhibits FZD5/8-mediated Wnt signaling

Given that Wnt induces FZD5/8 endocytosis and degradation and that ZNRF3/RNF43-mediated FZD5/8 degradation relies on Wnt ligands, we hypothesized that ZNRF3/RNF43 may specifically inhibit FZD5/8-mediated Wnt signaling. To test this hypothesis, we knocked out both *FZD5* and *FZD8* in ZRDKO cells (ZRDKO-FZD5/8DKO) via the CRISPR/Cas9 system and verified the results via genomic sequencing and flow cytometry (**Figure 6A**, **Figure 6-Figure Supplement 2A**). Immunoblotting revealed that the depletion of *FZD5/8* in ZRDKO cells dramatically reduced cytosolic β-catenin levels (**Figure 6B**), which were restored by re-expressing FZD5 but not FZD7 (**Figure 6C**). Furthermore, stable overexpression of FZD5 but not FZD7 further elevated the cytosolic β-catenin level in ZRDKO cells (**Figure 6D**). Additionally, stable expression of RNF43 in HEK293A or U2OS cells had a minimal effect on Wnt3a-induced β-catenin accumulation; interestingly, coexpressing FZD5 but not FZD7 in RNF43-expressing cells increased the inhibitory effect of RNF43 on Wnt3a-induced β-catenin accumulation (**Figure 6E** and **F**, **Figure 6-figure supplement 1A-B**).

We also generated *FZD5/8* double-knockout HEK293A cells (FZD5/8DKO) via the CRISPR/Cas9 system and verified them via genomic sequencing and flow cytometry analysis (**Figure 6G**, **Figure 6-Figure supplement 2B**). Immunoblotting revealed that *FZD5/8* double knockout had little effect on Wnt3a-induced cytosolic β-catenin accumulation but dramatically abolished RSPO1-induced cytosolic β-catenin accumulation (**Figure 6H** and **I**), which was reversed by re-expressing FZD5 or FZD8 in FZD5/8DKO cells (**Figure 6J-K**).

Collectively, these findings indicate that RSPO1 enhances Wnt signaling primarily through FZD5/8, whereas ZNRF3/RNF43 specifically inhibits Wnt signaling mediated by FZD5/8.

Wnt induces FZD5 and RNF43 interaction

As Wnt ligands induce ZNRF3/RNF43-dependent FZD5/8 degradation, we hypothesized that these ligands may also promote interactions between FZD5/8 and ZNRF3/RNF43 at the plasma membrane. To test this hypothesis, we utilized a proximity biotin labeling technique, which is well suited for detecting inducible and transient interactions (Branon et al., 2018; Li et al., 2023a). To minimize interference from endogenous ZNRF3/RNF43, we employed HEK293A ZRDKO cells stably expressing V5-FZD5-mTB or V5-FZD7-mTB (with miniTurbo biotin ligase fused to the carboxyl terminus of FZD5 or FZD7) alongside RNF43ΔRING-HA (lacking the enzymatic RING domain of RNF43). We confirmed the expression of FZD5/7-mTB and RNF43ΔRING, as well as the biotinylation efficiency, through immunoblotting (**Figure 7A**). We subsequently conducted proximity biotin labeling assays with or without Wnt3a, Wnt5a, or IWP-2 treatment. Both Wnt3a and Wnt5a significantly increased the biotinylation of RNF43ΔRING in FZD5-mTB-expressing cells but not in FZD7-mTB-expressing cells (**Figure 7B**). Additionally, IWP-2 treatment reduced the basal biotinylation of RNF43ΔRING in FZD5-mTB-expressing cells (**Figure 7B**). We further replicated the proximity labeling assay in DVLTKO cells, and the results revealed that DVL proteins

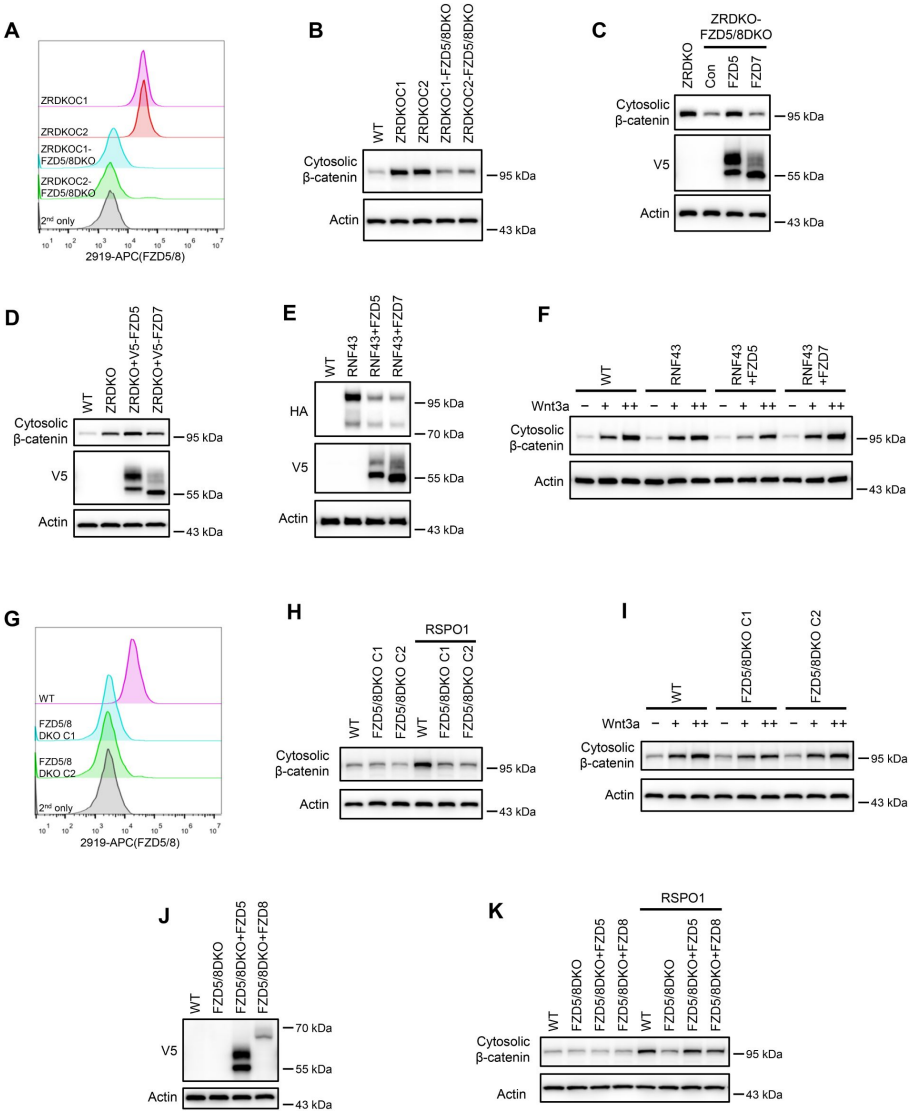

Figure 6.

ZNRF3/RNF43 specifically inhibits FZD5/8-mediated Wnt signaling, whereas RSPO1 specifically potentiates FZD5/8-mediated Wnt signaling.

(A) Flow cytometry analysis of FZD5/8 levels on the cell surface in ZRDKO and ZRDKO-FZD5/8DKO cells with an anti-FZD5/8 antibody.
(B) Depletion of FZD5/8 diminished the increase in cytosolic β-catenin levels in ZRDKO cells. Cytosolic fractions from the indicated cells were analyzed by immunoblotting.
(C) Re-expression of V5-FZD5, but not V5-FZD7, restored cytosolic β-catenin levels in ZRDKO-FZD5/8DKO cells.
(D) Overexpressing V5-FZD5, but not V5-FZD7, further elevated cytosolic β-catenin level in ZRDKO cells.
(E, F) FZD5, but not FZD7, enhanced the inhibitory effect of RNF43 on Wnt3a signaling. HEK293A cells stably expressing RNF43-HA alone or with V5-FZD5 or V5-FZD7 were treated with increasing doses of Wnt3a for 2 hours, and the cytosolic fractions were analyzed by immunoblotting.
(G) Flow cytometry analysis of cell surface FZD5/8 levels in WT or FZD5/8DKO cells.
(H, I) *FZD5/8* double knockout abolished RSPO1-induced cytosolic β-catenin accumulation but had little effect on Wnt3a-induced increases in cytosolic β-catenin levels. The cells were treated with RSPO1 CM for 4 hours (G) or increasing doses of Wnt3a for 2 hours (H), and the cytosolic fractions were analyzed by immunoblotting.
(J) WCLs from WT, FZD5/8DKO and FZD5/8DKO cells stably expressing V5-FZD5 or V5-FZD8 were analyzed by immunoblotting.
(K) *FZD5/8* double knockout abolished RSPO1-induced cytosolic β-catenin accumulation, which was restored by re-expressing V5-FZD5 or V5-FZD8.

did not participate in the Wnt3a- or Wnt5a-induced FZD5−RNF43 interaction (**Figure 7-figure supplement 1A–B**). These results suggest that Wnt induces DVL-independent interactions between FZD5 and RNF43 at the plasma membrane.

Discussion

Our results demonstrate that Wnt signaling employs a strategy analogous to that of receptor–tyrosine kinase pathways, where ligands bind to and activate receptors while simultaneously inducing receptor endocytosis and degradation to modulate signaling strength and duration (Alexander, 1998; Sorkin and Waters, 1993). Our results also illuminate the mechanism by which RSPO-ZNRF3/RNF43 regulates Wnt-induced FZD5/8 endocytosis and degradation and its influence on Wnt signaling. In the presence of ZNRF3/RNF43, Wnt binds to FZD5/8, forming a complex with ZNRF3/RNF43 and facilitating FZD5/8 endocytosis and subsequent lysosomal degradation, and this process occurs independently of DVL proteins. In the absence of ZNRF3/RNF43, Wnt still induces FZD5/8 endocytosis; however, endosomes harboring FZD5/8 fail to merge with lysosomes, leading to the accumulation of mature FZD5/8 within the cell, which may be recycled back to the plasma membrane for reuse to sustain signaling activity (**Figure 7C**).

There are ten FZD proteins in mammals that are classified into five subfamilies on the basis of their sequence similarity. Among them, FZD5/8 was reported to have higher signaling activity and broader Wnt binding and response spectrum (Martin et al., 2022; Wang et al., 2016). A recent study suggested that FZD5 undergoes maturation through specific binding to cholesterol (Zheng et al., 2022). Our current study suggests that Wnt specifically induces FZD5/8 endocytosis and degradation, adding a new feature to the FZD5/8 subfamily. Wnt-induced FZD5/8 endocytosis relies on the CRD domain and is dispensable for the FZD5/8 intracellular carboxyl terminus. It is possible that the Wnt-FZD5/8 complex recruits another unidentified membrane protein that promotes the internalization of the whole complex. Wnt3a and Wnt5a bind to FZD5/8, FZD4, and FZD7 with similar affinities (Li et al., 2023b) and specifically induce FZD5/8 but not other FZDs endocytosis. Therefore, further characterization and comparison of the structural differences between Wnt-bound CRDs from different FZDs and identification of specific binding proteins of the Wnt-FZD5/8 complex will shed light on the underlying mechanism. Although we showed that Wnt3a, Wnt5a, and endogenously expressed Wnts in 293A cells specifically induce FZD5/8 endocytosis, we cannot exclude the possibility that other Wnts or ligands may induce the endocytosis and degradation of other FZDs in certain biological contexts.

Our results also shed light on the function of DVL proteins in FZD endocytosis. We showed that FZD receptors undergo ligand-independent constant endocytosis that relies on DVL. However, Wnt-induced FZD5/8 endocytosis and degradation occur in the absence of DVL proteins. A previous study reported that DVL proteins interact with ZNRF3/RNF43 and may transport ZNRF3/RNF43 to FZD, thus facilitating FZD endocytosis and degradation (Jiang et al., 2015). Notably, these results are largely based on flow cytometry assays, which can detect only the internalization but not the degradation of FZDs. Furthermore, they used a ZNRF3/RNF43ΔDIR-DEP fusion protein and showed that expressing this fusion protein efficiently removed FZD proteins from the cell surface. Notably, the DEP domain of DVL also interacts with FZDs, and the ZNRF3/RNF43ΔDIR-DEP fusion protein may function as an anti-FZD “PROTAC” to degrade FZDs. Our results indicated that Wnt-induced FZD5/8 degradation requires ZNRF3/RNF43 but is dispensable for DVL proteins, suggesting that the interaction between DVL and ZNRF3/RNF43 is not required for this process. We cannot exclude the possibility that ZNRF3/RNF43 may regulate ligand-independent FZD endocytosis and degradation under certain circumstances that may rely on the DVL-ZNRF/RNF43 interaction. It is also possible that DVL interacts with ZNRF3/RNF43 to regulate ZNRF3/RNF43 endocytosis. Our results also revealed that overexpressing the membrane

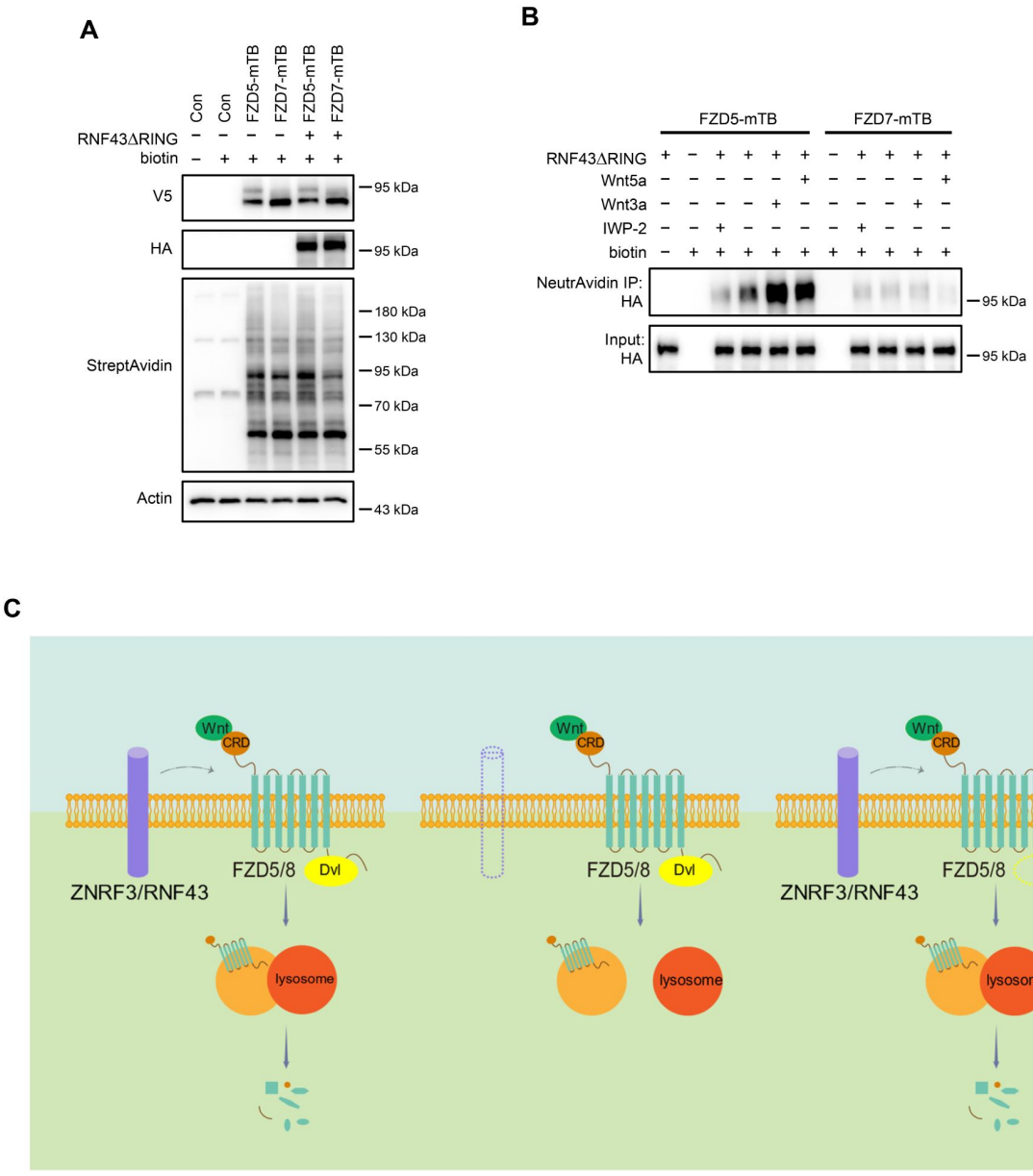

Figure 7.

Wnt3a and Wnt5a induce the FZD5–RNF43 interaction.

(A) Verification of protein expression and biotinylation efficiency in HEK293A ZRDKO cells stably expressing V5-FZD5-mTB or V5-FZD7-mTB alone or together with RNF43ΔRING-HA. The cells were treated with or without biotin (200 μM) and analyzed by immunoblotting with the indicated antibodies.
(B) Wnt3a or Wnt5a induces interaction between FZD5 and RNF43△RING but not FZD7. The cells in (A) were treated with IWP-2, control, Wnt3a or Wnt5a conditional medium with or without biotin as indicated, and the WCLs were precipitated with NeutrAvidin agarose beads, followed by immunoblotting analysis.
(C) Schematic model of Wnt-induced FZD5/8 endocytosis and degradation. In the presence of ZNRF3/RNF43, Wnt binds to FZD5/8 and forms a complex with ZNRF3/RNF43, leading to FZD5/8 endocytosis and subsequent lysosomal degradation. This process is not affected by the absence of DVL proteins. In the absence of ZNRF3/RNF43, Wnt still induces FZD5/8 endocytosis; however, endosomes containing FZD5/8 do not merge with lysosomes, resulting in the accumulation of mature FZD5/8 intracellularly.

RING-type E3 ligases RNF130 and RNF150 reduced membrane FZD levels without affecting cytosolic β-catenin levels, suggesting potential nonspecific effects of ZNRF3/RNF43 in overexpression assays.

Our results suggest that ZNRF3/RNF43 regulates the degradation of internalized FZD5/8 but is not required for Wnt-induced FZD5/8 internalization. Wnt can still induce FZD5 internalization in the absence of ZNRF3/RNF43, and internalized FZD5 accumulates on intracellular vesicles in both ZRDKO cells and WT cells treated with RSPO1. It is well established that internalized membrane proteins are sorted in endosomes either for recycling or for lysosomal degradation (Cullen and Steinberg, 2018). The ubiquitination of intracellular lysine residues serves as a typical sorting signal that can be recognized by the endosomal sorting complexes required for transport (ESCRT) and sorted for lysosomal degradation (Cullen and Steinberg, 2018). It is conceivable that ZNRF3/RNF43 ubiquitinates FZD5/8 during Wnt-induced FZD5/8 endocytosis and that the internalized ubiquitinated FZD5/8 is then sorted for lysosomal degradation. In the absence of ZNRF3/RNF43 or with RSPO treatment, internalized FZD5/8 is not ubiquitinated and thus is sorted for recycling. However, further investigations are needed to elucidate the detailed mechanism of the intracellular vesicular trafficking of internalized FZDs.

Our results suggest that RSPO-ZNRF3/RNF43 specifically targets Wnt-bound FZD5/8, as *FZD5/8* double knockout largely abolished Wnt/β-catenin signaling activity in ZRDKO cells or WT cells treated with RSPO1. Our results provide an underlying mechanism for a recent study in which the authors reported that FZD5, but not the other FZDs, is crucial for the growth of RNF43-mutated pancreatic tumors and colorectal tumor organoids (Steinhart et al., 2017). This mechanism may be crucial for stem cell self-renewal and tissue homeostasis. RSPO proteins, known as stem cell factors, are present in stem cell niches (de Lau et al., 2011; Yan et al., 2017), while ZNRF3/RNF43 are also expressed in stem cells (Koo et al., 2012; Sato et al., 2011; Yan et al., 2017). FZD5 is expressed in adult stem cells and is essential for their function (Alsaadi et al., 2023; Harada et al., 2021; Nabhan et al., 2023; Yan et al., 2017; Zheng et al., 2022).

In summary, our study introduces a novel concept in Wnt signaling regulation at the FZD receptor level, clarifies the mechanisms by which RSPO-ZNRF3/RNF43 regulates Wnt signaling, and offers new insights into Wnt signaling-related regenerative medicine and cancer therapy.

Methods

Reagents and tools table

Reagent or Resource	Source	Catalog Number or Identifier
Antibodies		
Rabbit monoclonal anti-HA	Cell Signaling Technology	Cat# 3724; RRID:AB_1549585
Rabbit monoclonal anti-V5	Cell Signaling Technology	Cat# 13202; RRID:AB_2687461
Mouse monoclonal anti-V5	Cell Signaling Technology	Cat# 80076; RRID:AB_2920661
Rabbit polyclonal anti-Beta Catenin	Proteintech	Cat# 51067-2-AP; RRID:AB_2086128
Rabbit polyclonal anti-DVL1	Proteintech	Cat# 27384-1-AP; RRID:AB_2880859
Mouse monoclonal anti-DVL2	Proteintech	Proteintech Cat# 67105-1-Ig; RRID:AB_2882409
Rabbit polyclonal anti-DVL3	Proteintech	Cat# 13444-1-AP; RRID:AB_2093451
Rabbit monoclonal anti-ACTB	ABclonal	Cat# AC026; RRID:AB_2768234
Rabbit monoclonal anti-LAMP1	Cell Signaling Technology	Cat# 9091; RRID:AB_2687579
Mouse monoclonal anti-EEA1	Cell Signaling Technology	Cat# 48453, RRID:AB_2920538
Alexa Fluor 488 AffiniPure Donkey anti-Rabbit IgG (H+L)	Yeasen Biotech	Cat# 34206ES60; RRID:AB_2909605

Alexa Fluor 488 AffiniPure Donkey Anti-Mouse IgG(H+L)	Yeasen Biotech	Cat# 34106ES60; RRID:AB_2920874
Alexa Fluor 647 AffiniPure Donkey anti-Rabbit IgG (H+L)	Yeasen Biotech	Cat# 34213ES60
Alexa Fluor 647 AffiniPure Donkey Anti-Mouse IgG(H+L)	Yeasen Biotech	Cat# 34113ES60
Allophycocyanin-AffiniPure F(ab')2 Fragment Goat Anti-Rabbit IgG (H+L)	Jackson ImmunoResearch Labs	Cat# 111-136-144; RRID:AB_2337987
Allophycocyanin-AffiniPure F(ab')2 Fragment Goat Anti-Mouse IgG (H+L)	Jackson ImmunoResearch Labs	Cat# 115-136-146; RRID:AB_2338651
Peroxidase-AffiniPure Goat Anti-Rabbit IgG (H+L)	Jackson ImmunoResearch Labs	Cat# 111-035-003; RRID:AB_2313567
HRP-conjugated goat anti-mouse IgG (H+L)	Mabnus	Cat# GS80002
HRP-labeled Streptavidin	Beyotime	Cat# A0303
Pierce NeutrAvidin Agarose	Thermo Fisher Scientific	Cat# 29201
Mouse monoclonal anti-pan-FZD (OMP-18R5)	(Stagg and Dupont, 2014)	N/A
Mouse monoclonal anti-FZD5/8 (2919)	(Pan et al., 2021)	N/A
Mouse monoclonal anti-FZD4 (5028)	(Sachdev Sidhu, 2021)	N/A
Bacterial strand		
Trelief® 5α Chemically Competent Cell	Tsingke	Cat# TSC-C01
Chemicals		
IWP-2	Sigma–Aldrich	Cat# I0536
D-Biotin	Sigma–Aldrich	Cat# B4639
Polyethylenimine (PEI)	Polysciences	Cat# 19850
Puromycin	Solarbio	Cat# P8230
Hygromycin	Yeasen Biotech	Cat# 60225ES03
G418 Sulfate	Yeasen Biotech	Cat# 60220ES03
Digitonin	Yeasen Biotech	Cat# 54004ES25
NP-40	Yeasen Biotech	Cat# 20103ES60
Triton X-100	Sangon Biotech	Cat# A600198

4% Paraformaldehyde Fix Solution	Sangon Biotech	Cat# E672002
Propidium iodide (PI)	Sangon Biotech	Cat# A601112
Potassium chloride (KCl)	Sangon Biotech	Cat# A610440
Sodium carbonate (Na_2CO_3)	Sangon Biotech	Cat# A100585
Urea	Sangon Biotech	Cat# A600148
Bafilomycin A1 (BA1)	Selleck	Cat# S1413
Protease Inhibitor Cocktail	Selleck	Cat# B14001
Phosphatase Inhibitor Cocktail	Selleck	Cat# B15001
EZ-link Sulfo-NHS-SS-Biotin	Thermo Fisher Scientific	Cat# 21331
Critical commercial assays/kits		
Phanta Max Super-Fidelity DNA Polymerase	Vazyme	Cat# P505-d1
2 × Taq Plus Master Mix	Vazyme	Cat# P212-01
Gel Extraction Kit	CWBIO	Cat# CW2302M
EndoFree Plasmid Mini Kit	CWBIO	Cat# CW2106S
Seamless Cloning Kit	Beyotime	Cat# D7010S
Experimental Models: Cell Lines		
HEK293T	ATCC	Cat# CRL-11268
HEK293A	Procell	Cat# CL-0003
Huh7	Procell	Cat# CL-0120
MCF7	Procell	Cat# CL-0149
769P	Procell	Cat# CL-0009
U2OS	ATCC	Cat# HTB-96
L cell	ATCC	Cat# CRL-2648
L-Wnt3a cell	ATCC	Cat# CRL-2647
L-Wnt5a cell	ATCC	Cat# CRL-2814

Recombinant DNA		
pCDH-CMV-hyg-V5-FZD1	This paper	N/A
pCDH-CMV-hyg-V5-FZD2	This paper	N/A
pCDH-CMV-hyg-V5-FZD3	This paper	N/A
pCDH-CMV-hyg-V5-FZD4	This paper	N/A
pCDH-CMV-hyg-V5-FZD5	This paper	N/A
pCDH-CMV-hyg-V5-FZD6	This paper	N/A
pCDH-CMV-hyg-V5-FZD7	This paper	N/A
pCDH-CMV-hyg-V5-FZD8	This paper	N/A
pCDH-CMV-hyg-V5-FZD9	This paper	N/A
pCDH-CMV-hyg-V5-FZD10	This paper	N/A
pCDH-CMV-hyg-V5- FZD5△CRD	This paper	N/A
pCDH-CMV-hyg-V5-FZD5△C	This paper	N/A
pCDH-CMV-hyg-V5-FZD4CRD-FZD5	This paper	N/A
pCDH-CMV-hyg-V5-FZD5CRD-FZD4	This paper	N/A
pCDH-CMV-hyg-V5-FZD7CRD-FZD5	This paper	N/A
pCDH-CMV-hyg-V5-FZD5CRD-FZD7	This paper	N/A
pUC19-FZD5KI-donor	This paper	N/A
LentiCRISPRv2-FZD5KI-sgRNA	This paper	N/A
pUC19-FZD7KI-donor	This paper	N/A
LentiCRISPRv2-FZD7KI-sgRNA	This paper	N/A
LentiCRISPRv2-ZNRF3KO-sgRNA	(Jiang et al., 2015)	N/A
LentiCRISPRv2-RNF43KO-sgRNA	(Jiang et al., 2015)	N/A
LentiCRISPRv2-DVL1KO-sgRNA	(Jiang et al., 2015)	N/A

LentiCRISPRv2-DVL2KO-sgRNA	This paper	N/A
LentiCRISPRv2-DVL3KO-sgRNA	This paper	N/A
pCDH-CMV-hyg-V5- linker-FZD5	This paper	N/A
pCDH-CMV-hyg-V5- linker-FZD7	This paper	N/A
pCDH-CMV-puro-DVL2	This paper	N/A
pCDH-CMV-puro-ZNRF3-HA	This paper	N/A
pCDH-CMV-puro-RNF43-HA	This paper	N/A
pCDH-CMV-puro-RNF130-HA	This paper	N/A
pCDH-CMV-puro-RNF150-HA	This paper	N/A
LentiCRISPRv2-FZD5KO-sgRNA	This paper	N/A
LentiCRISPRv2-FZD8KO-sgRNA	This paper	N/A
pCS2+-RSPO1-Flag	This paper	N/A
pCDH-CMV-hyg-V5-FZD5-mTB	(Li et al., 2023a)	N/A
pCDH-CMV-hyg-V5-FZD7-mTB	(Li et al., 2023a)	N/A
pCDH-CMV-puro-RNF43△RING-HA	This paper	N/A
psPAX2	Addgene	Cat# 12260
pMD2.G	Addgene	Cat# 12259

Cell culture

HEK293T, HEK293A, Huh7, MCF7, 769P, U2OS and mouse L cells stably expressing Wnt3a or Wnt5a were cultured in high-glucose Dulbecco's modified Eagle's medium (boster) supplemented with 10% fetal bovine serum (Genial) and 1% penicillin/streptomycin at 37°C in a humidified incubator (Thermo Fisher Scientific) with 5% CO_2.

Generation of CRISPR/Cas9 knockout (KO) cell lines

HEK293A cells were transfected with LentiCRSIPRv2 plasmids encoding Cas9 and guide RNAs via PEI transfection reagents. Forty-eight hours posttransfection, the cells were selected with puromycin (1 μg/mL). Following selection, the cells were plated at a density of 500 cells per 10 cm dish to facilitate the growth of monoclonal cell lines. Once colonies had formed, they were gently harvested by pipetting and subsequently verified via genomic DNA sequencing. Additionally, *FZD5/8* double knockout (FZD5/8DKO) clones were confirmed via flow cytometry with an anti-FZD5/8 (2919) monoclonal antibody.

Generation of KI cell lines

HEK293A cells were transfected with donor plasmids along with LentiCRSIPRv2 knock-in plasmids via PEI transfection reagents. Selection was performed with puromycin (1 μg/mL) 48 hours posttransfection. The cells were then further selected with G418 sulfate (1 mg/mL) for 7 days. Monoclonal cell lines were established by seeding the selected cells in 10 cm dishes. After colony

formation, the cells were harvested by pipetting and verified by immunoblotting. The sequences for the knock-in sgRNAs were as follows: FZD5KI (GGTGTCCCTGTCGCACGTGT) and FZD7KI (CAGCAGCAAGGGGGGGAGACTG).

Plasmids

V5-FZD1-10 (in which a V5 tag was inserted after the signal peptide) was cloned and inserted into the pCDH lentiviral vector, which included a hygromycin resistance gene, and ZNRF3-HA, RNF43-HA, RNF130-HA and RNF150-HA (in which an HA tag was inserted at the C-terminus) were cloned and inserted into the pCDH lentiviral vector, which included a puromycin resistance gene. V5-FZD5△CRD (missing amino acids 31--172) and FZD5△C (missing amino acids 524-−585) were generated using full-length FZD5 as the template. FZD5CRD-FZD4, FZD5CRD-FZD7 were made by combining FZD5CRD with FZD4△CRD (missing amino acids 42--167) or FZD7 △CRD (missing amino acids 45--169), FZD4CRD-FZD5, and FZD7CRD-FZD5 were made by combining FZD4CRD or FZD7CRD with FZD5△CRD. V5-FZD5/FZD7-mTB plasmids were generated by inserting miniTurbo biotin ligase at the C-terminus of V5-FZD5/FZD7. The V5-linker-FZD5/7 was generated by inserting a linker sequence between V5 and FZD5/7 to extend the distance between the V5 tag and the FZD protein. RSPO1 was tagged with a Flag epitope at its C-terminus. RNF43ΔRING (missing amino acids 270–316) was generated using full-length RNF43 as the template. FZD5/7KI donors were constructed with the following elements sequentially connected: the left homologous arm with the stop codon replaced by a V5 tag, a P2A peptide, a G418 resistance gene, and the right homologous arm. The sequences targeted by the LentiCRISPRv2 sgRNA are detailed in the expanded view figures. All plasmids were confirmed by Sanger sequencing.

Conditioned medium

Wnt3a- and Wnt5a-conditioned media were generated according to the ATCC's product sheet. L-Wnt3a or L-Wnt5a cells were cultured at an appropriate density in 10 cm dishes. After 4 days, the medium was collected, and the cells were replenished with fresh medium for an additional 3 days. The medium was then collected again. Medium harvested from L wild-type cells was used as a control. For RSPO1 production, HEK293T cells were transfected with an RSPO1 expression plasmid, and the culture medium was changed 24 hours posttransfection. The supernatant containing the secreted proteins was collected after an additional 24 hours. Media harvested from HEK293T cells transfected with empty pCS2+ plasmids served as controls. All the collected media were subsequently centrifuged at 12000 × g for 20 minutes at 4°C to remove cellular debris, after which their activity was tested by immunoblotting before use.

Lentivirus packaging and stable cell line generation

HEK293T cells were seeded in 6 cm dishes to achieve approximately 50% confluency and were transfected with a total of 3 μg of plasmid, consisting of 1.5 μg of the overexpression vector, 1 μg of psPAX2 and 0.5 μg of pMD2.G. Sixteen hours posttransfection, the medium of the cells was replaced with supplemented DMEM. The virus-containing medium was harvested 48 hours and 72 hours after transfection and then filtered through 0.22 μm filters.

For the generation of stable cell lines, HEK293A or U2OS cells were seeded in 6 cm dishes. A mixture of lentivirus-containing medium with fresh medium was added to the cells. Twenty-four hours post infection, the medium was replaced with DMEM containing 10% FBS. After an additional 24 h, the cells were transferred to 10 cm dishes and selected with puromycin (1 μg/mL) or hygromycin (250 μg/mL) to isolate resistant cells.

Immunoblotting

The cells were seeded in 12-well plates and treated under the indicated conditions. Following treatment, the cells were washed with PBS, lysed with 2 × protein loading buffer (125 mM Tris–HCl pH 6.8, 2% SDS, 10% glycerol, 0.004% bromophenol blue, and 8% β-mercaptoethanol) and

boiled for 10 minutes at 95°C. For detection of FZD proteins, the cells were lysed with 0.5% NP-40 lysis buffer containing protease inhibitor cocktail for 30 minutes with gentle rotation at 4°C. The lysates were collected in 1.5 mL tubes and centrifuged at 12000 × g for 15 minutes at 4°C. The supernatants were then harvested and mixed with 5 × protein loading buffer. Note that the lysates intended for detecting FZD proteins should not be boiled. Cytosolic fractions were extracted using 0.015% digitonin in PBS containing a protease inhibitor cocktail for 10 minutes with gentle rotation at 4°C. The fractions were centrifuged, and the supernatants were mixed with 5 × protein loading buffer and then boiled for 10 minutes at 95°C.

Protein samples were separated by denaturing electrophoresis on 6%-10% SDS−PAGE gels (Epizyme) and transferred to 0.45 μm PVDF membranes (Millipore) via a wet transfer system (Tanon). The membranes were blocked with TBST containing 5% nonfat dry milk at room temperature for 1 hour and then incubated with primary antibodies overnight at 4°C. After being washed with TBST, the membranes were incubated with secondary antibodies for 1 hour at room temperature. Following additional washes with TBST to remove unbound antibodies, specific protein bands were detected via an enhanced chemiluminescence (ECL)-immunoblotting system (GelView 6000Pro II, BLT Photon Technology).

Flow Cytometry

HEK293A cells were incubated with ice-cold PBS for 10 min with gentle rotation at 4°C, and Huh7, MCF7 and 769P cells were washed with PBS once and incubated with PBS containing 2 mM EDTA for 10 min at 4°C. Then, the cells were collected in 1.5 mL tubes via gentle pipetting. The harvested cells were subsequently centrifuged at 400 × g for 2 minutes at 4°C. After the supernatants were removed, the pellets were resuspended and incubated with the indicated primary antibodies diluted in FACS buffer (5% goat serum in PBS) for 1 hour on ice. The cells were then washed with ice-cold PBS, centrifuged, and incubated with secondary antibodies for an additional hour on ice. Following another wash with PBS, the cells were stained with propidium iodide (PI) and analyzed via a NovoCyte Quanteon flow cytometer (Agilent). PI-negative cells are displayed in histogram plots.

Cell surface biotinylation assay

To detect cell surface levels of endogenous FZD5, HEK293A FZD5KI cells were washed with PBS and incubated with the EZ-linker sulfo-NHS-SS-biotin in PBS for 10 min on ice. The unbound reagent was removed by washing with PBS, and the cells were then treated with the indicated CM for 2 hours at 37°C in a humidified incubator. Thereafter, the cells were washed with PBS and lysed with 0.5% NP-40 lysis buffer containing protease inhibitor cocktail for 30 minutes with gentle rotation at 4°C. The lysates were collected in 1.5 mL tubes and centrifuged at 12000 × g for 15 minutes at 4°C. The supernatants were then harvested and incubated with NeutrAvidin agarose beads overnight. The beads were subsequently centrifuged at 1500 × g for 2 min, washed 6 times with lysis buffer and eluted with 2 × protein loading buffer containing 8% β-mercaptoethanol for 30 min at room temperature. Cell surface proteins were detected by immunoblotting.

Immunofluorescence

The cells were seeded on circular microscope cover glasses and treated under the indicated conditions. Following treatment, the cells were fixed with 4% paraformaldehyde (PFA) for 30 minutes at room temperature. After fixation, the cells were permeabilized with 0.1% TX-100 in PBS for 20 minutes at room temperature with gentle rotation. The cells were then blocked with 5% donkey serum in PBS for 1 hour at room temperature. Primary antibodies (diluted in 5% donkey serum) were applied overnight at 4°C. The cells were washed with PBS and incubated with fluorescently labeled secondary antibodies for 1 hour at room temperature with gentle rotation. After being washed, the cells were stained with DAPI for 5 minutes at room temperature and analyzed via a confocal microscope (LSM 980 with Airyscan 2, ZEISS).

To detect FZD5/7 endocytosis in HEK293A cells, the indicated cells were seeded and treated with IWP-2 overnight. The cells were incubated with anti-V5 antibody diluted in fresh culture medium for 1 h at 4°C and then washed with PBS to remove unbound antibody. The cells were subsequently treated with control or Wnt5a conditional medium for 1 h in a humidified incubator at 37°C with 5% CO2. The cells were fixed and permeabilized after treatment, incubated with secondary antibodies, washed with PBS and stained with DAPI.

Biotin labeling with miniTurbo

HEK293A ZRDKO cells stably expressing V5-FZD5-mTB or V5-FZD7-mTB, either alone or together with RNF43ΔRING-HA, were treated with IWP-2, control CM, Wnt3a CM, or Wnt5a CM with or without biotin (200 μM) as indicated. Following treatment, the cells were washed with PBS to remove unbound biotin and lysed in lysis buffer (25 mM Tris-HCl (pH 7.4), 150 mM NaCl, 1% NP-40, 1% sodium deoxycholate, 0.6% SDS) containing a protease inhibitor cocktail. The cell lysates were boiled for 10 min at 98°C and centrifuged at 12000 × g for 15 min. The supernatants were harvested and incubated with NeutrAvidin agarose beads (Thermo Fisher Scientific) overnight. The beads were then centrifuged at 1500 × g for 2 min, washed twice with lysis buffer, once with 1 M KCl, once with 0.1 M Na_2CO_3, once with 2 M urea (diluted in 10 mM Tris-HCl, pH 8.0), and twice with lysis buffer. Specific proteins were eluted with 2 × protein loading buffer containing 10 mM biotin and boiled for 10 minutes at 95°C. The eluted protein samples were subsequently analyzed by immunoblotting.

Statistical Analyses

For quantification of the number of FZD5 and FZD7 puncta in WT, DVLTKO and DVLTKO + DVL2 HEK293A cells, images were acquired via a confocal microscope (LSM 980 with Airyscan 2, ZEISS). Punctate structures of FZD proteins in 20 cells per cell line were counted via ImageJ software (NIH Image). To quantify colocalization, Mander's coefficients for FZD5 puncta overlapping with LAMP1 or EEA1 puncta were calculated via ImageJ. Statistical analyses were performed via two-tailed unpaired Student's t tests, and the results are presented as the means ± SDs and were analyzed via GraphPad Prism 8. Statistical significance was defined as follows: ns (no significant difference, $p > 0.05$), *** ($p < 0.001$), **** ($p < 0.0001$).

Acknowledgements

This research was supported by a grant from the National Natural Science Foundation of China (81870620 to XZ), by funding from Sichuan Provincial People's Hospital (to XZ), and by the National Institutes of Health (R01GM57603 (completed) and R35GM134953/MIRA to XH).

Additional information

Author contributions

Conceptualization: D. Luo and X. Zhang. Investigation: D. Luo, J. Zheng and S. Lv. Funding acquisition: X. Zhang and X. He. Supervision: X. Zhang and X. He. Writing – original draft: X. Zhang, D. Luo and J. Zheng. Writing – review and editing: X. Zhang, D. Luo, R. Sheng, M. Chen and X. He.

Funding

National Natural Science Foundation of China (81870620)

Figure 1-Figure supplement 1.

Wnt induces FZD5/8 endocytosis and degradation.

(A) Wnt3a or Wnt5a specifically reduced the cell surface levels of V5-FZD5/8 in Huh7 cells. Huh7 cells stably expressing each of the 10 V5-FZDs (FZD1 to 10) were treated with control, Wnt3a, or Wnt5a CM for 4 hours, and the cell surface levels of V5-FZDs were analyzed via flow cytometry using an anti-V5 antibody.
(B) Wnt3a or Wnt5a specifically decreased the levels of mature forms of V5-FZD5 in U2OS cells. The whole-cell lysates (WCLs) from the indicated U2OS cells treated as described in (A) were analyzed by immunoblotting with the indicated antibodies.

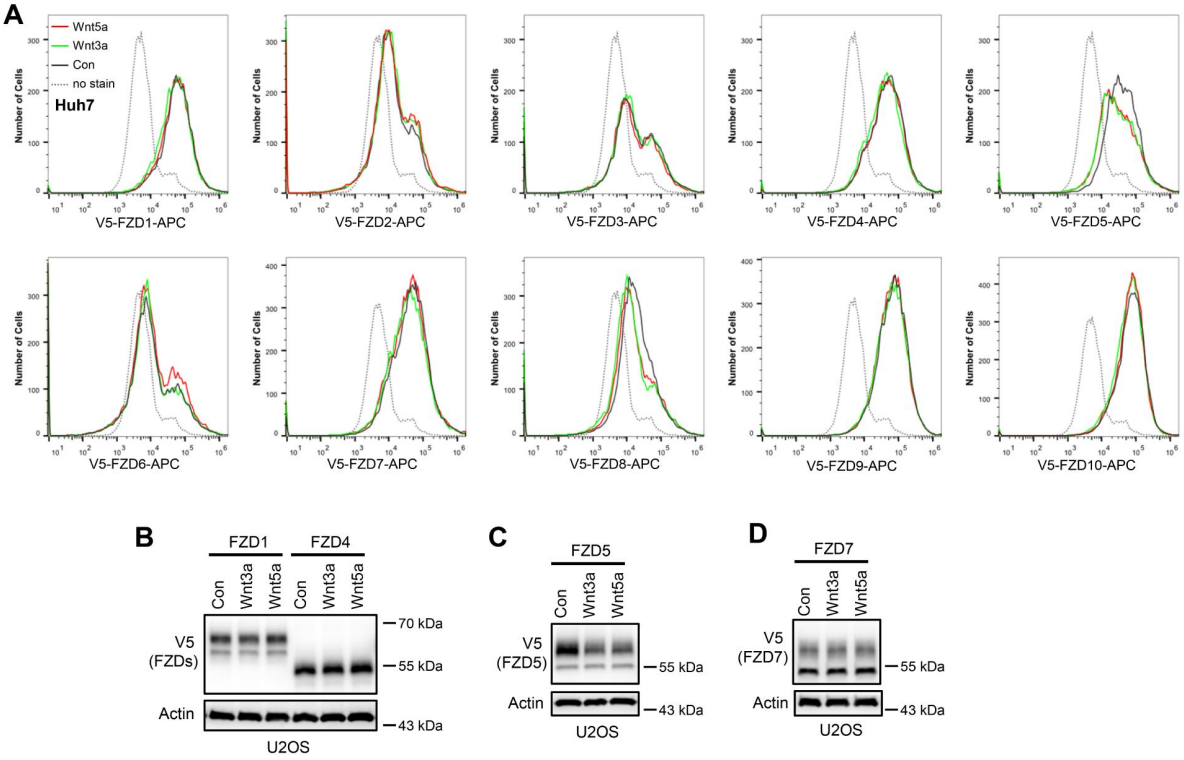

Figure 2-Figure supplement 1.

IWP-2 increased the cell surface levels of endogenous FZD5/8 in several cell lines.

(A-C) IWP-2 increased the cell surface levels of endogenous FZD5/8 in Huh7 (A), MCF7 (B) and 769P (C) cells. The indicated cells were treated with or without IWP-2 and analyzed by flow cytometry to determine the FZD5/8 levels on the cell surface with anti-FZD5/8 (2919) monoclonal antibodies. APC, allophycocyanin.

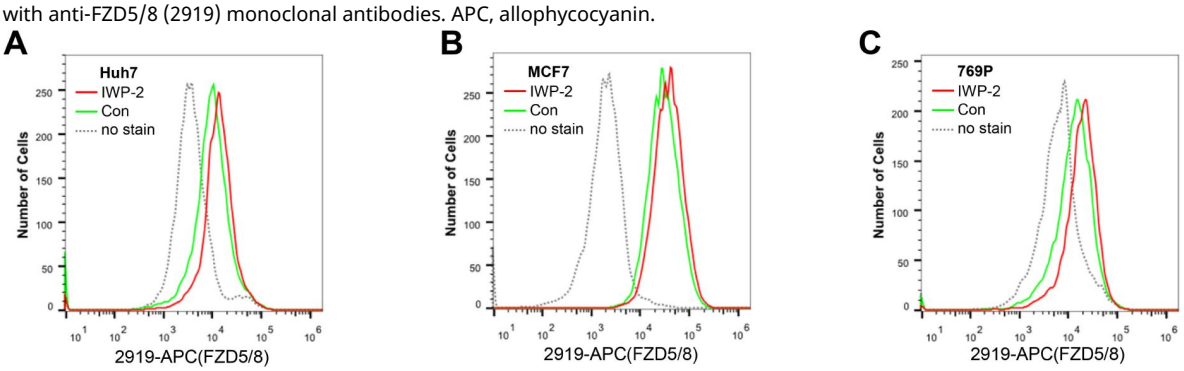

Figure 2-Figure supplement 2.

Characterization of the antibodies used for flow cytometry in this study.

HEK293A WT cells or cells stably expressing each of the 10 V5-FZDs were analyzed by flow cytometry with the indicated antibodies.

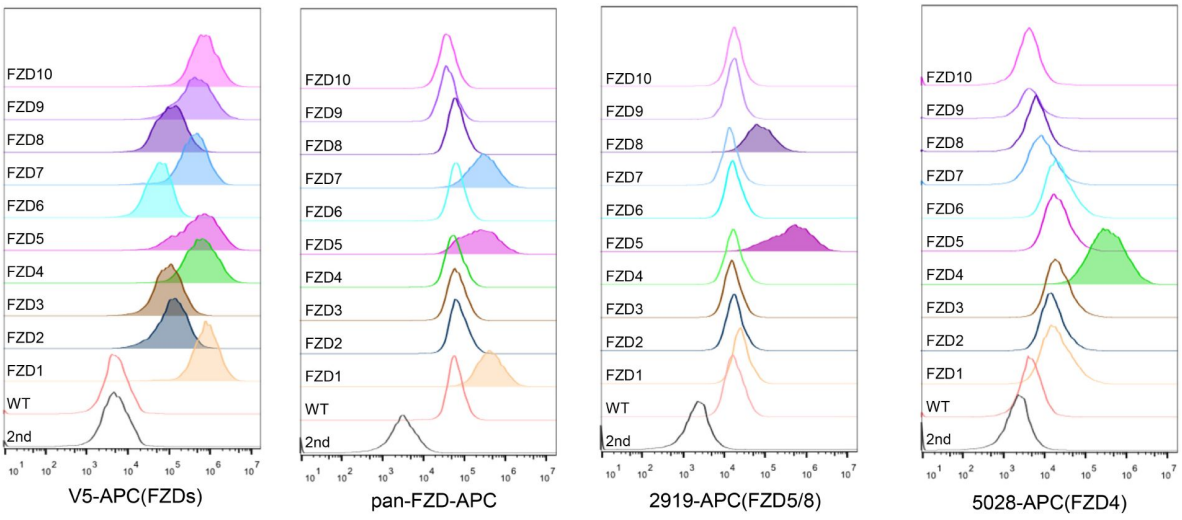

Figure 2-Figure supplement 3.

Genetic lesions in ZRDKO cells.

Genomic DNA sequencing results showing mutations in *ZNRF3* and *RNF43* in ZRDKO clones. The reference nucleotide sequence (WT allele) is presented at the top. The sequences targeted by the sgRNA are highlighted in red, with cleavage sites indicated by red arrows.

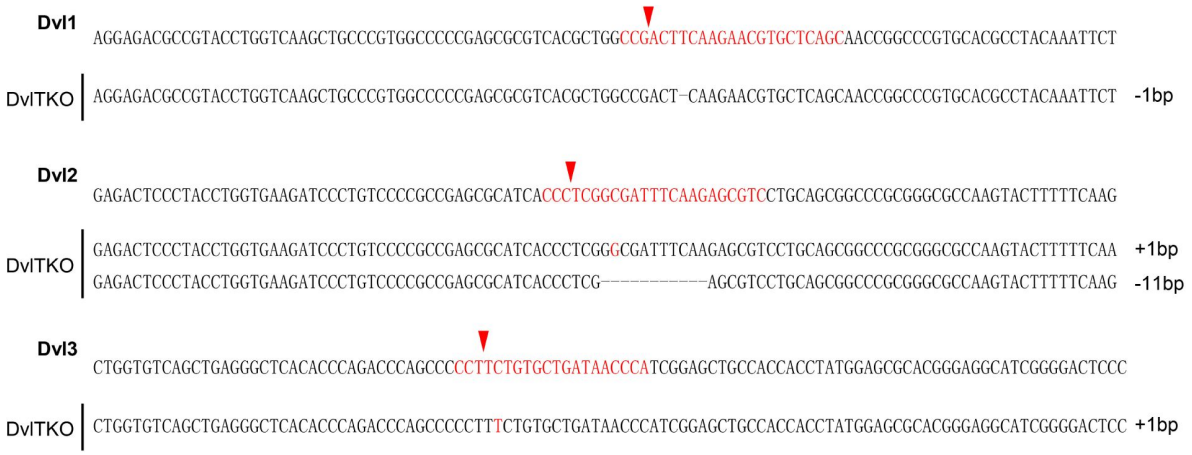

Figure 3-Figure supplement 1.

Genetic lesions in DVLTKO cells.

Genomic DNA sequencing results showing mutations in *DVL1*, *DVL2* and *DVL3* in the DVLTKO clone. The reference nucleotide sequence (WT allele) is presented at the top. The sequences targeted by the sgRNA are highlighted in red, with cleavage sites indicated by red arrows.

Figure 4-Figure supplement 1.

ZNRF3/RNF43 is required for the degradation of Wnt3a-induced internalized FZD5.

(A) Wnt3a induced FZD5 internalization in both WT and ZRDKO cells, and internalized FZD5 gradually diminished in WT but not ZRDKO cells. WT or ZRDKO cells stably expressing V5-FZD5 were treated with control or Wnt3a CM for the indicated times and analyzed by immunostaining. The cells were treated with IWP-2 overnight prior to treatment with CM. Scale bars, 10 μm.
(B) Cotreatment with RSPO1 prevented FZD5 degradation but had little effect on FZD5 internalization induced by Wnt3a. The cells were treated with IWP-2 overnight prior to treatment with CM. Scale bars, 10 μm.

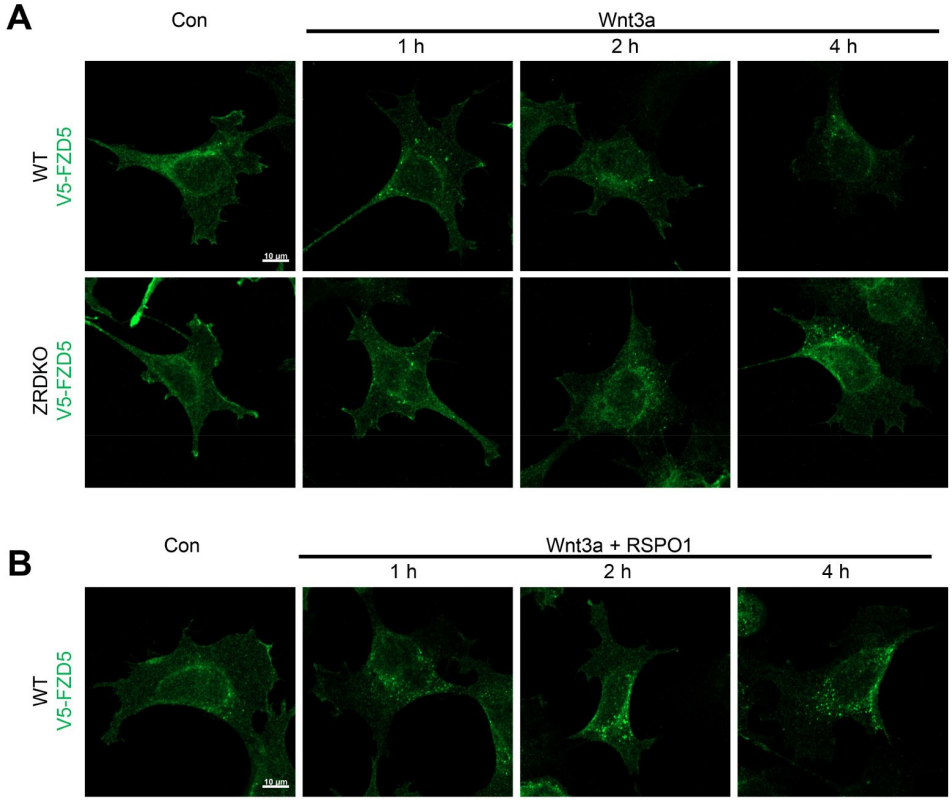

Figure 6-Figure supplement 1.

RNF43 specifically regulates FZD5/8-mediated Wnt signaling in U2OS cells.

(A) U2OS cells stably expressing RNF43-HA alone or together with V5-FZD5 or V5-FZD7 were analyzed by immunoblotting with the indicated antibodies to confirm protein expression.
(B) Cells in (A) were treated with increasing doses of Wnt3a for 2 hours, and the cytosolic fractions were analyzed by immunoblotting. Notably, the expression of FZD5, but not FZD7, enhanced the inhibitory effect of RNF43 on Wnt3a signaling.

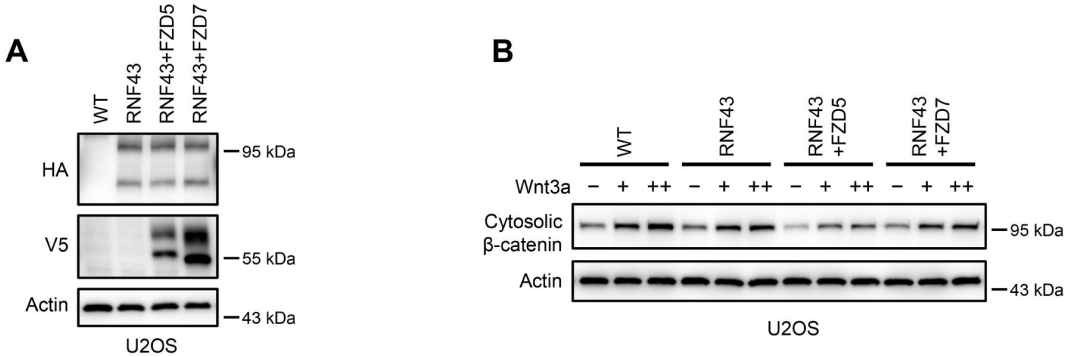

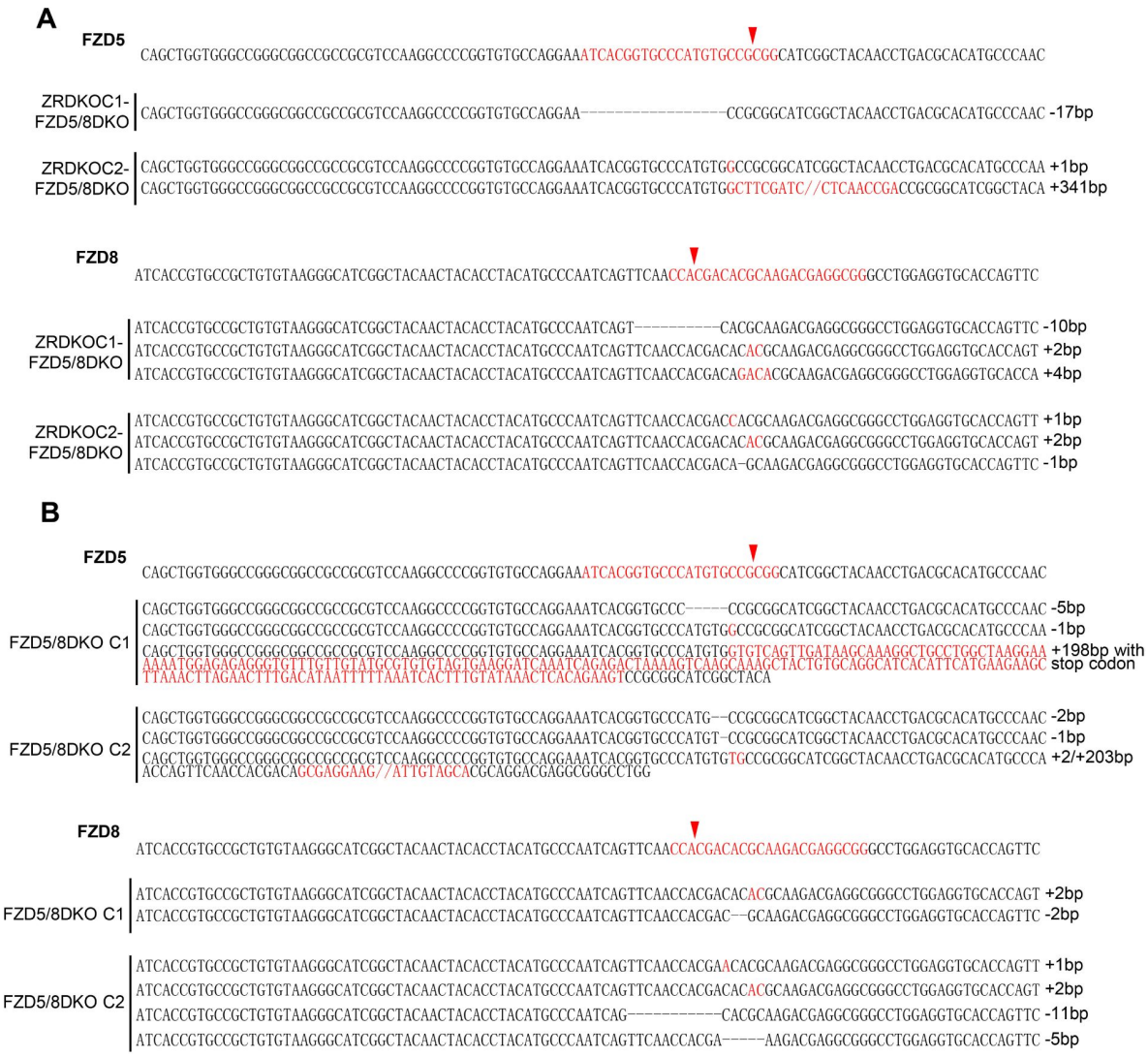

Figure 6-Figure supplement 2.

Genetic lesions in ZRDKO-FZD5/8DKO and FZD5/8DKO cells.

(A, B) Genomic DNA sequencing results showing mutations in *FZD5* and *FZD8* in the ZRDKO-FZD5/8DKO (A) and FZD5/8DKO clones (B). The reference nucleotide sequence (WT allele) is presented at the top. The sequences targeted by the sgRNA are highlighted in red, and the cleavage sites are indicated by red arrows.

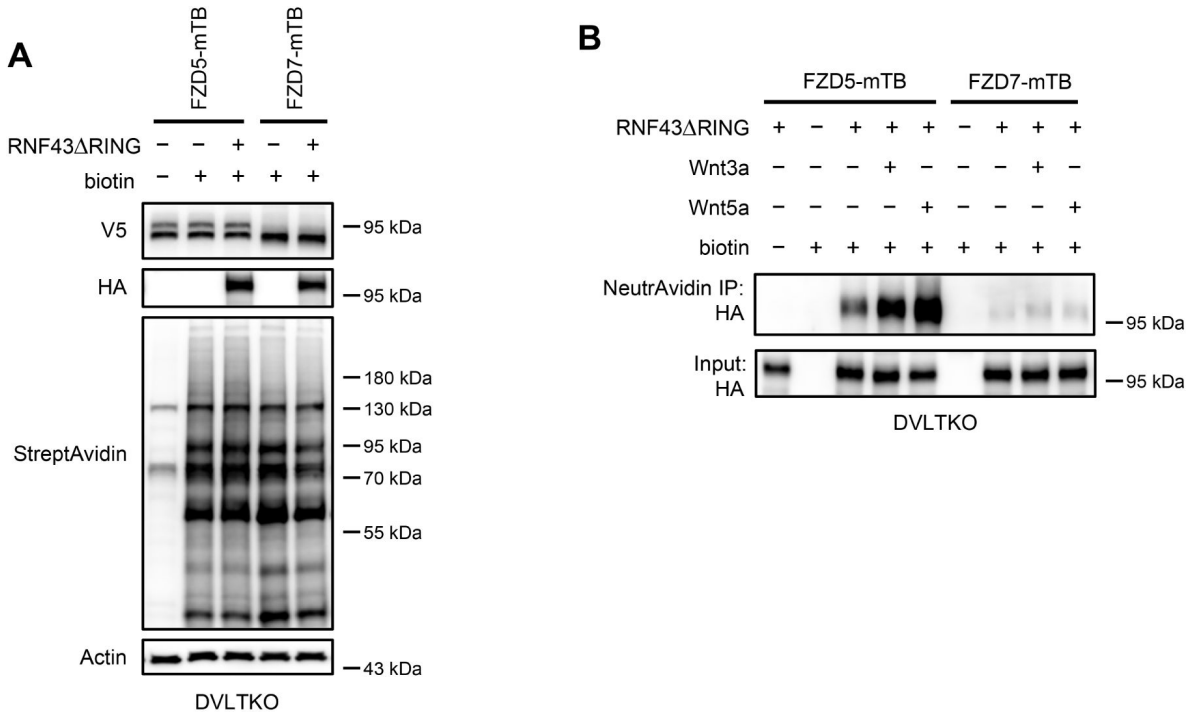

Figure 7-Figure supplement 1.

Wnt3a and Wnt5a induce the FZD5−RNF43 interaction in DVLTKO cells.

(A) Verification of protein expression and biotinylation efficiency in HEK293A DVLTKO cells stably expressing V5-FZD5-mTB or V5-FZD7-mTB alone or together with RNF43ΔRING-HA. The cells were treated with or without biotin (200 μM) and analyzed by immunoblotting with the indicated antibodies.
(B) Wnt3a or Wnt5a induces an interaction between FZD5 and RNF43△RING but not FZD7 in DVLTKO cells. The cells in (A) were treated with control, Wnt3a or Wnt5a conditional medium with or without biotin as indicated, and the WCLs were precipitated with NeutrAvidin agarose beads, followed by immunoblotting analysis.

References

Alexander A (1998) **Endocytosis and intracellular sorting of receptor tyrosine kinases** *Front Biosci* **3**:d729–738 Google Scholar

Alsaadi A., Artibani M., Hu Z., Wietek N., Morotti M., Gonzalez L.S., Alazzam M., Jiang J., Abdul B., Soleymani Majd H., Blazer L.L., Adams J., Silvestri F., Sidhu S.S., Brugge J.S., Ahmed A.A. (2023) **Single-cell transcriptomics identifies a WNT7A-FZD5 signaling axis that maintains fallopian tube stem cells in patient-derived organoids** *Cell Rep* **42**:113354 Google Scholar

Anastas J.N., Moon R.T. (2013) **WNT signalling pathways as therapeutic targets in cancer** *Nat Rev Cancer* **13**:11–26 Google Scholar

Branon T.C., Bosch J.A., Sanchez A.D., Udeshi N.D., Svinkina T., Carr S.A., Feldman J.L., Perrimon N., Ting A.Y. (2018) **Efficient proximity labeling in living cells and organisms with TurboID** *Nat Biotechnol* **36**:880–887 Google Scholar

Bugter J.M., Fenderico N., Maurice M.M. (2021) **Mutations and mechanisms of WNT pathway tumour suppressors in cancer** *Nat Rev Cancer* **21**:5–21 Google Scholar

Bugter J.M., van Kerkhof P., Jordens I., Janssen E., Tran Ngoc Minh T., Iglesias van Montfort D., Jamieson C., Maurice M.M. (2024) **E3 ligases RNF43 and ZNRF3 display differential specificity for endocytosis of Frizzled receptors** *Life Sci Alliance* **7** Google Scholar

Chen M., Amado N., Tan J., Reis A., Ge M., Abreu J.G., He X. (2020) **TMEM79/MATTRIN defines a pathway for Frizzled regulation and is required for Xenopus embryogenesis** *eLife* **9** Google Scholar

Chen W., ten Berge D., Brown J., Ahn S., Hu L.A., Miller W.E., Caron M.G., Barak L.S., Nusse R., Lefkowitz R.J. (2003) **Dishevelled 2 recruits beta-arrestin 2 to mediate Wnt5A-stimulated endocytosis of Frizzled 4** *Science* **301**:1391–1394 Google Scholar

Clevers H., Nusse R. (2012) **Wnt/beta-catenin signaling and disease** *Cell* **149**:1192–1205 Google Scholar

Cullen P.J., Steinberg F. (2018) **To degrade or not to degrade: mechanisms and significance of endocytic recycling** *Nat Rev Mol Cell Biol* **19**:679–696 Google Scholar

de Lau W., Barker N., Low T.Y., Koo B.K., Li V.S., Teunissen H., Kujala P., Haegebarth A., Peters P.J., van de Wetering M., Stange D.E., van Es J.E., Guardavaccaro D., Schasfoort R.B., Mohri Y., Nishimori K., Mohammed S., Heck A.J., Clevers H. (2011) **Lgr5 homologues associate with Wnt receptors and mediate R-spondin signalling** *Nature* **476**:293–297 Google Scholar

Dubey R., van Kerkhof P., Jordens I., Malinauskas T., Pusapati G.V., McKenna J.K., Li D., Carette J.E., Ho M., Siebold C., Maurice M., Lebensohn A.M., Rohatgi R. (2020) **R-spondins engage heparan sulfate proteoglycans to potentiate WNT signaling** *eLife* **9** Google Scholar

Farnhammer F., Colozza G., Kim J. (2023) **RNF43 and ZNRF3 in Wnt Signaling - A Master Regulator at the Membrane** *Int J Stem Cells* **16**:376–384 Google Scholar

Haglund K., Dikic I. (2012) **The role of ubiquitylation in receptor endocytosis and endosomal sorting** *J Cell Sci* **125**:265–275 Google Scholar

Hao H.X., Jiang X., Cong F. (2016) **Control of Wnt Receptor Turnover by R-spondin-ZNRF3/RNF43 Signaling Module and Its Dysregulation in Cancer** *Cancers (Basel)* **8** Google Scholar

Hao H.X., Xie Y., Zhang Y., Charlat O., Oster E., Avello M., Lei H., Mickanin C., Liu D., Ruffner H., Mao X., Ma Q., Zamponi R., Bouwmeester T., Finan P.M., Kirschner M.W., Porter J.A., Serluca F.C., Cong F. (2012) **ZNRF3 promotes Wnt receptor turnover in an R-spondin-sensitive manner** *Nature* **485**:195–200 Google Scholar

Harada S., Mabuchi Y., Kohyama J., Shimojo D., Suzuki S., Kawamura Y., Araki D., Suyama T., Kajikawa M., Akazawa C., Okano H., Matsuzaki Y. (2021) **FZD5 regulates cellular senescence in human mesenchymal stem/stromal cells** *Stem Cells* **39**:318–330 Google Scholar

Huang H.C., Klein P.S. (2004) **The Frizzled family: receptors for multiple signal transduction pathways** *Genome Biol* **5**:234 Google Scholar

Jiang X., Charlat O., Zamponi R., Yang Y., Cong F. (2015) **Dishevelled promotes Wnt receptor degradation through recruitment of ZNRF3/RNF43 E3 ubiquitin ligases** *Mol Cell* **58**:522–533 Google Scholar

Jiang X., Cong F. (2016) **Novel Regulation of Wnt Signaling at the Proximal Membrane Level** *Trends Biochem Sci* **41**:773–783 Google Scholar

Kazanskaya O., Glinka A., del Barco Barrantes I., Stannek P., Niehrs C., Wu W. (2004) **R-Spondin2 is a secreted activator of Wnt/beta-catenin signaling and is required for Xenopus myogenesis** *Dev Cell* **7**:525–534 Google Scholar

Koo B.K., Spit M., Jordens I., Low T.Y., Stange D.E., van de Wetering M., van Es J.H., Mohammed S., Heck A.J., Maurice M.M., Clevers H. (2012) **Tumour suppressor RNF43 is a stem-cell E3 ligase that induces endocytosis of Wnt receptors** *Nature* **488**:665–669 Google Scholar

Lebensohn A.M., Rohatgi R. (2018) **R-spondins can potentiate WNT signaling without LGRs** *eLife* **7** Google Scholar

Li M., Zheng J., Luo D., Xu K., Sheng R., MacDonald B.T., He X., Zhang X. (2023a) **Frizzled receptors facilitate Tiki inhibition of Wnt signaling at the cell surface** *EMBO Rep* **24**:e55873 Google Scholar

Li M.Y., Zheng J., Luo D., Xu K., Sheng R., MacDonald B.T., He X., Zhang X.J. (2023b) **Frizzled receptors facilitate Tiki inhibition of Wnt signaling at the cell surface** *Embo Reports* **24** Google Scholar

Marmor M.D., Yarden Y. (2004) **Role of protein ubiquitylation in regulating endocytosis of receptor tyrosine kinases** *Oncogene* **23**:2057–2070 Google Scholar

Martin M., Vermeiren S., Bostaille N., Eubelen M., Spitzer D., Vermeersch M., Profaci C.P., Pozuelo E., Toussay X., Raman-Nair J., Tebabi P., America M., De Groote A., Sanderson L.E., Cabochette P., Germano R.F.V., Torres D., Boutry S., de Kerchove d'Exaerde A., Bellefroid E.J.,

Phoenix T.N., Devraj K., Lacoste B., Daneman R., Liebner S., Vanhollebeke B. (2022) **Engineered Wnt ligands enable blood-brain barrier repair in neurological disorders** *Science* **375**:eabm4459 Google Scholar

Nabhan A.N., Webster J.D., Adams J.J., Blazer L., Everrett C., Eidenschenk C., Arlantico A., Fleming I., Brightbill H.D., Wolters P.J., Modrusan Z., Seshagiri S., Angers S., Sidhu S.S., Newton K., Arron J.R., Dixit V.M. (2023) **Targeted alveolar regeneration with Frizzled-specific agonists** *Cell* **186**:2995–3012 Google Scholar

Niehrs C (2012) **The complex world of WNT receptor signalling** *Nat Rev Mol Cell Biol* **13**:767–779 Google Scholar

Nusse R., Clevers H. (2017) **Wnt/beta-Catenin Signaling, Disease, and Emerging Therapeutic Modalities** *Cell* **169**:985–999 Google Scholar

O'Brien S., Chidiac R., Angers S. (2023) **Modulation of Wnt-beta-catenin signaling with antibodies: therapeutic opportunities and challenges** *Trends Pharmacol Sci* **44**:354–365 Google Scholar

Pan G., Moffat J., Sidhu S., Angers S., Steinhart Z., Wang X. (2021) **Frizzled5 protein-binding agents. Patent US10919968B2** *United States*

Park S., Wu L., Tu J., Yu W., Toh Y., Carmon K.S., Liu Q.J. (2020) **Unlike LGR4, LGR5 potentiates Wnt-beta-catenin signaling without sequestering E3 ligases** *Sci Signal* **13** Google Scholar

Rim E.Y., Clevers H., Nusse R. (2022) **The Wnt Pathway: From Signaling Mechanisms to Synthetic Modulators** *Annu Rev Biochem* **91**:571–598 Google Scholar

Sachdev Sidhu G.P., Moffat Jason, Angers Stephane, Steinhart Zachary, Pavlovic Zvezdan, Adams Jarrett (2021) **Frizzled receptor antibodies and uses thereof. Patent WO2021026652A9** *United States*

Sato T., van Es J.H., Snippert H.J., Stange D.E., Vries R.G., van den Born M., Barker N., Shroyer N.F., van de Wetering M., Clevers H. (2011) **Paneth cells constitute the niche for Lgr5 stem cells in intestinal crypts** *Nature* **469**:415–418 Google Scholar

Sorkin A., Waters C.M. (1993) **Endocytosis of growth factor receptors** *Bioessays* **15**:375–382 Google Scholar

Stagg R.J., Dupont J. (2014) **Methods of treating neuroendocrine tumors using frizzled-binding agents. Patent US20140134159A1** *United States*

Stapornwongkul K.S., Vincent J.P. (2021) **Generation of extracellular morphogen gradients: the case for diffusion** *Nat Rev Genet* **22**:393–411 Google Scholar

Steinhart Z., Angers S. (2018) **Wnt signaling in development and tissue homeostasis** *Development* **145** Google Scholar

Steinhart Z., Pavlovic Z., Chandrashekhar M., Hart T., Wang X., Zhang X., Robitaille M., Brown K.R., Jaksani S., Overmeer R., Boj S.F., Adams J., Pan J., Clevers H., Sidhu S., Moffat J., Angers S. (2017) **Genome-wide CRISPR screens reveal a Wnt-FZD5 signaling circuit as a druggable vulnerability of RNF43-mutant pancreatic tumors** *Nat Med* **23**:60–68 Google Scholar

Szenker-Ravi E., Altunoglu U., Leushacke M., Bosso-Lefevre C., Khatoo M., Thi Tran H., Naert T., Noelanders R., Hajamohideen A., Beneteau C., de Sousa S.B., Karaman B., Latypova X., Basaran S., Yucel E.B., Tan T.T., Vlaminck L., Nayak S.S., Shukla A., Girisha K.M., Le Caignec C., Soshnikova N., Uyguner Z.O., Vleminckx K., Barker N., Kayserili H., Reversade B. (2018) **RSPO2 inhibition of RNF43 and ZNRF3 governs limb development independently of LGR4/5/6** *Nature* **557**:564–569 Google Scholar

Tsukiyama T., Fukui A., Terai S., Fujioka Y., Shinada K., Takahashi H., Yamaguchi T.P., Ohba Y., Hatakeyama S. (2015) **Molecular Role of RNF43 in Canonical and Noncanonical Wnt Signaling** *Mol Cell Biol* **35**:2007–2023 Google Scholar

Tsukiyama T., Koo B.K., Hatakeyama S. (2021) **Post-translational Wnt receptor regulation: Is the fog slowly clearing?: The molecular mechanism of RNF43/ZNRF3 ubiquitin ligases is not yet fully elucidated and still controversial** *Bioessays* **43**:e2000297 Google Scholar

Wang Y., Chang H., Rattner A., Nathans J. (2016) **Frizzled Receptors in Development and Disease** *Curr Top Dev Biol* **117**:113–139 Google Scholar

Xie Y., Zamponi R., Charlat O., Ramones M., Swalley S., Jiang X., Rivera D., Tschantz W., Lu B., Quinn L., Dimitri C., Parker J., Jeffery D., Wilcox S.K., Watrobka M., LeMotte P., Granda B., Porter J.A., Myer V.E., Loew A., Cong F. (2013) **Interaction with both ZNRF3 and LGR4 is required for the signalling activity of R-spondin** *EMBO Rep* **14**:1120–1126 Google Scholar

Yamamoto H., Komekado H., Kikuchi A. (2006) **Caveolin is necessary for Wnt-3a-dependent internalization of LRP6 and accumulation of beta-catenin** *Dev Cell* **11**:213–223 Google Scholar

Yan K.S., Janda C.Y., Chang J., Zheng G.X.Y., Larkin K.A., Luca V.C., Chia L.A., Mah A.T., Han A., Terry J.M., Ootani A., Roelf K., Lee M., Yuan J., Li X., Bolen C.R., Wilhelmy J., Davies P.S., Ueno H., von Furstenberg R.J., Belgrader P., Ziraldo S.B., Ordonez H., Henning S.J., Wong M.H., Snyder M.P., Weissman I.L., Hsueh A.J., Mikkelsen T.S., Garcia K.C., Kuo C.J. (2017) **Non-equivalence of Wnt and R-spondin ligands during Lgr5(+) intestinal stem-cell self-renewal** *Nature* **545**:238–242 Google Scholar

Yu A., Rual J.F., Tamai K., Harada Y., Vidal M., He X., Kirchhausen T. (2007) **Association of Dishevelled with the clathrin AP-2 adaptor is required for Frizzled endocytosis and planar cell polarity signaling** *Dev Cell* **12**:129–141 Google Scholar

Zhang C., Lai M.B., Khandan L., Lee L.A., Chen Z., Junge H.J. (2017) **Norrin-induced Frizzled4 endocytosis and endo-lysosomal trafficking control retinal angiogenesis and barrier function** *Nat Commun* **8**:16050 Google Scholar

Zheng S., Lin J., Pang Z., Zhang H., Wang Y., Ma L., Zhang H., Zhang X., Chen M., Zhang X., Zhao C., Qi J., Cao L., Wang M., He X., Sheng R. (2022) **Aberrant Cholesterol Metabolism and Wnt/beta-Catenin Signaling Coalesce via Frizzled5 in Supporting Cancer Growth** *Adv Sci (Weinh)* **9**:e2200750 Google Scholar

Author information

Dong Luo*
Key Laboratory of Molecular Biophysics of the Ministry of Education, College of Life Science and Technology, Huazhong University of Science and Technology, Wuhan, China, The Sichuan Provincial Key Laboratory for Human Disease Gene Study and Department of Laboratory Medicine, Center for Medical Genetics, Sichuan Provincial People's Hospital, School of Medicine, University of Electronic Science and Technology of China, Chengdu, China

*These authors contributed equally to this work

Jing Zheng*
Key Laboratory of Molecular Biophysics of the Ministry of Education, College of Life Science and Technology, Huazhong University of Science and Technology, Wuhan, China, The Sichuan Provincial Key Laboratory for Human Disease Gene Study and Department of Laboratory Medicine, Center for Medical Genetics, Sichuan Provincial People's Hospital, School of Medicine, University of Electronic Science and Technology of China, Chengdu, China

*These authors contributed equally to this work

Shuning Lv
Key Laboratory of Molecular Biophysics of the Ministry of Education, College of Life Science and Technology, Huazhong University of Science and Technology, Wuhan, China, The Sichuan Provincial Key Laboratory for Human Disease Gene Study and Department of Laboratory Medicine, Center for Medical Genetics, Sichuan Provincial People's Hospital, School of Medicine, University of Electronic Science and Technology of China, Chengdu, China

Ren Sheng
College of Life and Health Science, Northeastern University, Shenyang, China
ORCID iD: 0000-0002-2293-8986

Maorong Chen
Center for Life Sciences, School of Life Sciences, Yunnan University, Kunming, China
ORCID iD: 0000-0003-3744-8864

Xi He
The F. M. Kirby Neurobiology Center, Boston Children's Hospital, Department of Neurology, Harvard Medical School, Boston, United States
ORCID iD: 0000-0002-8093-7981

Xinjun Zhang
Key Laboratory of Molecular Biophysics of the Ministry of Education, College of Life Science and Technology, Huazhong University of Science and Technology, Wuhan, China, Research Unit for Blindness Prevention of the Chinese Academy of Medical Sciences (2019RU026), Sichuan Academy of Medical Sciences and Sichuan Provincial People's Hospital, Chengdu, China, The Sichuan Provincial Key Laboratory for Human Disease Gene Study and Department of Laboratory Medicine, Center for Medical Genetics, Sichuan Provincial People's Hospital, School of Medicine, University of Electronic Science and Technology of China, Chengdu, China
ORCID iD: 0000-0003-2409-4104

For correspondence: xzhang@uestc.edu.cn

Editors

Reviewing Editor
Yi Arial Zeng
Chinese Academy of Sciences, Shanghai, China

Senior Editor
Volker Dötsch
Goethe University Frankfurt, Frankfurt am Main, Germany

Reviewer #1 (Public review):

Summary:

The mechanism by which WNT signals are received and transduced into the cell has been the topic of extensive research. Cell surface levels of the WNT receptors of the FZD family are subject to tight control and it's well established that the transmembrane ubiquitin ligases ZNRF3 and RNF43 target FZDs for degradation and that proteins of the R-spondin family block this effect. This manuscript explores the role that WNT proteins play in receptor internalization, recycling and degradation, and the authors provide evidence that WNTs promote interactions of FZD with the ubiquitin ligases. Using cells mutant in all 3 DVL genes, the authors demonstrate that this effect of WNT on FZD is DVL-independent.

Strengths:

Overall, the data are of good quality and support the authors' hypothesis. Strengths of this study is the use of CRISPR-mutated cell lines to establish genetic requirements for the various components. The finding that FZD internalization and degradation is WNT dependent and does not involve DVL is novel.

Weaknesses:

A weakness of the work includes a heavy reliance on overexpression of FZD proteins. To detect endogenous FZDs, the authors have inserted a V5 tag into the endogenous gene, which may affect their activity(ies).

https://doi.org/10.7554/eLife.103996.2.sa2

Reviewer #2 (Public review):

In this manuscript Luo et al uncover that the ZNRF3/RNF43 E3 ubiquitin ligases participate in the selective endocytosis and degradation of FZD5/8 receptors in response to Wnt stimulation. In my opinion there are three significant findings of this study: 1) Wnt proteins are required for ZNRF3/RNF43 mediated endocytosis and degradation of FZD receptors and this constitutes an important negative regulatory loop. 2) Wnt can induce FZD endocytosis in the absence of ZNRF3/RNF43 but this does not influence total or cell surface levels. 3) The ZNRF3/RNF43 substrate selectivity for FZD5/8 over the other 8 Frizzleds. Of course, many questions remain, and new ones emerge as it is often the case, but these findings challenge our dogmatic view on how the ZNRF3/RNF43 regulate Wnt signaling and emphasize their role in Wnt-dependent Frizzled endocytosis/degradation and beta-catenin signaling.

This is an elegant study employing several CRISPR-edited cell lines to tag endogenous Frizzled receptors and to knockout ZNRF3/RNF43 and all three Dishevelled proteins. One major strength of the study is therefore the careful assessment of the roles of RNF43 and ZNFR3 in

endogenous expression contexts. This is especially relevant since overexpression of membrane E3 ligases have been shown to ectopically degrade membrane proteins and could have blurred previous interpretations. A second strength is clarifying the role of Dishevelled proteins in FZD endocytosis. Indeed, although previous studies suggested that the Wnt-promoted interaction between FZD and RNF43/ZNFR3 was mediated through Dvl, the authors clearly show that this is not the case (using Dvl knockout cells and functional assays). Dvl proteins, on the other han,d are still required for ligand-independent FZD-endocytosis.

The only weakness pertains to the difference in signaling outcome, comparing elevated signaling seen when FZD levels are upregulated following ZNFR3/RNF43 KO vs ectopic overexpression. Indeed, the authors suggest that in the absence of RNF43/ZNFR3 the receptors could be recycled back to the PM and thereby contribute to increased signaling seen in the mutant cells. This has not been directly demonstrated.

https://doi.org/10.7554/eLife.103996.2.sa1

Author response:

The following is the authors' response to the original reviews.

> ***Reviewer #1 (Recommendations for the authors):***
>
> *Because many conclusions are drawn from overexpression studies and from a single cell line (HEK293), it is unclear how general these effects are. In particular, one of the main claims put forth in this manuscript is that of specificity, namely, that FZD5/8, and none of the other FZDs, are uniquely involved in this internalization and degradation. While there are examples of similar specificities, many of these examples can be attributed to a particular cellular context. Without demonstrating that this FZD5/8 specificity is observed in multiple cell lines and contexts, this point remains unconvincing and questionable. One way to address this point of criticism is to omit the word "specifically" in the title and soften the language concerning this idea throughout the manuscript.*

We appreciate your valuable comments and suggestions. We have removed the word "specifically" from the title and softened the language concerning this idea throughout the manuscript. Moreover, we performed new experiments to show that Wnt3a/5a induces FZD5/8 endocytosis and degradation and that IWP-2 treatment increases the cell surface levels of FZD5/8 in cell lines other than 293A (Figure 1-Figure supplement 1 and Figure 2-Figure supplement 1). These results indicate that Wnt-induced FZD5/8 endocytosis and degradation are not cell specific.

> *The starting point for these studies is a survey of all 10 FZDs, V5-tagged and overexpressed in HEK293 cells. Here, the authors observed a decline in cell surface levels of only FZD5 and 8 in response to Wnt3a and Wnt5a. As illustrated in the immunoblot (Fig 1B), several FZDs were poorly expressed, including FZD1, 3, 6 and 9, which calls into question that only FZD5 and 8 were affected. Furthermore, total levels of FZD8 don't diminish appreciably, as claimed by the authors, and only FZD5 shows a subtle decline upon WNT treatment. All of these experiments are performed with overexpressed V5-tagged FZD proteins or with endogenously V5-tagged (KI) proteins, and it is possible that overexpression or tagging lead to potentially artifactual observations. Examining the effects of WNTs on FZD protein localization and levels need to be done with endogenously expressed, non-tagged FZDs. In this context, it is somewhat puzzling that the authors don't show such an experiment using the pan- and FZD5/8-specific antibodies, which they use in multiple experiments throughout the manuscript. With these available tools it*

> *should be possible to examine FZD levels at the cell surface in response to Wnt3a and Wnt5a, ideally in multiple cell lines.*

We appreciate your valuable comments and suggestions. Figure 1B shows the results of the follow-up study shown in Figure 1A. As shown in Figure 1A, we used flow cytometry analysis to detect the cell surface levels of stably expressed FZDs and found that Wnt3a/5a specifically reduced the levels of FZD5/8 on the cell surface, suggesting that Wnt3a/5a induces FZD5/8 endocytosis. As shown in Figure 1B and C, we performed immunoblotting to examine whether Wnt3a/5a-induced FZD5/8 internalization resulted in FZD5/8 degradation. Notably, most FZDs exhibit two bands on immunoblots, as also suggested by other published studies, and the upper bands represent the mature form that is fully glycosylated and presented to the cell surface (see also new Figure 2L), whereas the lower bands represent the immature form. Our results clearly indicated that Wnt3a/5a treatment reduced the levels of the mature forms of both FZD5 and FZD8, although the immunoblotting signals of the mature form of FZD8 (upper bands) were relatively weak. The immunoblotting signals of the other FZDs varied, and some of them (including FZD1, -3, -6 and -9) were relatively weak; however, according to the results in Figure 1A, all of the FZDs were expressed and present on the cell surface.

Commercially available FZD5/8 antibodies, including those used in published studies, cannot detect endogenous FZD5/8 or can only recognize immature FZD5 in our hands, which is why we have to use the CRISPR-CAS9-based KI technique to introduce a V5 tag to FZD5 and FZD7. Notably, in the overexpression experiments, the V5 tag is on the amino terminus, and in the KI experiments, the V5 tag is on the carboxyl terminus of FZDs, which may minimize the potential artificial effects of the V5 tag on the immunoblotting assays.

The monoclonal antibodies used in this study, such as anti-pan-FZD, anti-FZD5/8, and anti-FZD4 antibodies, are neutralizing antibodies that can compete with Wnt ligands to bind to the FZD CRD. These antibodies have been successfully used to detect the surface levels of FZDs via flow cytometry assays. However, as the binding affinity of the Wnt-FZD CRD is comparable to the binding affinity of the antibody-FZD, we were cautious in using these antibodies to detect the cell surface levels of FZDs when the cells were treated with Wnt3a/5a CM, which contains relatively high concentrations of Wnt3a/5a. As shown in Author response image 1, Wnt3a or Wnt5a treatment dramatically reduced the endogenous cell surface level of FZD5/8, as detected by flow cytometry using the anti-FZD5/8 antibody. However, in another experiment, HEK293A cells were first incubated with cold Wnt3a or Wnt5a CM at 4°C to minimize endocytosis and then analyzed via flow cytometry using the anti-FZD5/8 antibody. The results showed that Wnt3a/5a incubation reduced the floe cytometry signals, suggesting that Wnt3a/5a binding to FZD5/8 might interfere with antibody-FZD5/8 binding, although we cannot exclude the possibility that Wnt3a/5a may induce FZD5/8 endocytosis at 4°C (Author response image 1).

Author response image 1.

(A) HEK293A cells were treated with control, Wnt3a or Wnt5a CM for 2 hours at 37°C in a humidified incubator and were analyzed via flow cytometry using the anti-FZD5/8 antibody.

(B) HEK293A cells were incubated with control, Wnt3a or Wnt5a CM for 1 h at 4°C and analyzed by flow cytometry using the anti-FZD5/8 antibody.

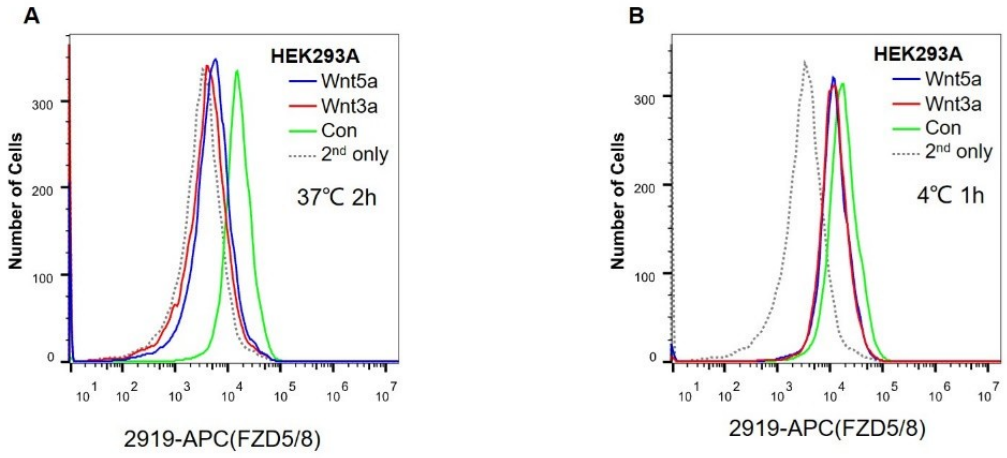

> *Several experiments rely on gene-edited clonal cell lines, including knockouts of FZD5/8, RNF43/ZNRF3, and DVL. Gene knockouts were confirmed by genomic DNA sequencing and, for DVL and FZD5/8, by loss of protein expression. While these KO lines are powerful tools to study gene function, there is a concern for clonal variability. Each cell line may have acquired additional changes as a result of gene editing. In addition, there may be compensatory changes in gene expression as a consequence of the loss of certain genes. For example, expression of other FZDs may increase in FZD5/8 DKO cells. To address this critique, the authors should show that re-expression of the knocked-out genes rescues the observed effect. This is done in some instances (Fig 5E, G, H) but not in other instances, such as with the DVL TKO (Fig. 3). Since the authors assert that DVL is important for FZD internalization in the absence of WNT, but not for FZD internalization in the presence of WNT, this particular rescue experiment is important. This is a potentially important finding and it should be confirmed by re-expression of DVL in the TKO line. As an alternative, conditional knockdown using Tet-inducible shRNA expression could address concerns for clonal variability.*

We appreciate your valuable comments and suggestions. We re-expressed DVL2 in DVLTKO cells stably expressing V5-linker-FZD5 or V5-linker-FZD7. As shown in Figure 3G-K, re-expression of DVL2 rescued the decreased Wnt-independent endocytosis of FZD5 and FZD7 caused by DVL1/2/3 knockout.

> *Given the significant differences in signaling activity by Wnt3a and Wnt5a, it is somewhat surprising that all experiments shown in this manuscript do not identify distinguishing features between Wnt3a and Wnt5a. In addition, it is unclear why the authors switch between Wnt3a and Wnt5a. For example, Figures 1C, 3G-J, 4C-D only use Wnt5a. In contrast, Figures 6E and H use Wnt3a, most likely because b-catenin stabilization is examined, an effect generally not observed with Wnt5a. The choice of which Wnt is examined/used appears to be somewhat arbitrary and the authors never provide any explanations for these choices. In the end, this type of inconsistency becomes puzzling when the authors present, quite convincingly, in Figure 7, that both Wnt3a and 5a promote an interaction between FZD5/8 and RNF43 through proximity biotin labeling.*

Although Wnt3a and Wnt5a are significantly different in triggering intracellular signaling pathways, both bind FZD5/8 and induce FZD5/8 endocytosis and degradation similarly. When FZD5 is stably overexpressed, Wnt5a has slightly stronger effects on inducing FZD5 endocytosis and degradation, possibly because the Wnt5a concentration may be higher than the Wnt3a concentration in our CM, which is why we used Wnt5a CM in some experiments

when V5-FZD5 was overexpressed. In the revised manuscript, we used both Wnt3a and Wnt5a CM in the experiments as you suggested, as shown in Figure 1C, 3G-K and Figure 4-Figure supplement 1.

> *Minor Points:*
>
> *Figure 3G and I: it is curious that individual cells are shown in the "0 h" samples, while the "Con 1 h" and "Wnt5a 1 h" show multiple cells with several making direct contact with each other. This is notable because the V5 staining at sites of cell-cell contact are quite distinct and variable between control and Wnt5a-treated and WT versus DVL TKO cells. Also, sub-cellular localization of FZD5 (V5 tag) puncta is quite distinct between Con and Wnt5a: puncta in Wnt5a-treated cells appear to be more plasma membrane proximal than in Con cells. These points may be easy to address by showing images of cells that are more similar with respect to cell number and density for each condition.*

Thank you for your suggestions. We repeated these experiments and added Wnt3a treatment and adjusted the cell density. Images including an individual cell were selected for presentation.

> *Figure 5E: the following statement is confusing/misleading: "Furthermore, reintroducing ZNRF3 or RNF43 into ZRDKO cells efficiently restored the increase in cytosolic β-catenin levels, whereas the expression of RNF130 or RNF150, two structurally similar transmembrane E3 ubiquitin ligases, did not (Fig. 5E)." First, reintroduction of ZNRF3 or RNF43 restores cytosolic b-catenin levels; it does not restore the increase in b-catenin. Second, the claim that RNF130 fails to have this effect is not substantiated since it is barely expressed.*

Thank you for your suggestions and comments. We reorganized the language to make the statement clearer. Notably, the expression level of RNF130 was relatively low compared with that of other E3 ligases, but RNF130 was expressed (Figure 5E darker exposure) and could reduce the cell surface levels of FZDs, as shown in Figure 5G.

> ***Reviewer #2 (Recommendations for the authors):***
>
> *(1) Given their results the authors conclude that upregulation of Frizzled on the plasma membrane is not sufficient to explain the stabilization of beta-catenin seen in the ZNRF3/RNF43 mutant cells. This interpretation is sound, and they suggest in the discussion that ZNRF3/RNF43-mediated ubiquitination could serve as a sorting signal to sort endocytosed FZD to lysosomes for degradation and that absence or inhibition of this process would promote FZD recycling. This should be relatively easy to test using surface biotinylation experiments and would considerably strengthen the manuscript.*

Thank you for your valuable suggestions and comments. We performed cell surface biotinylation experiments in HEK293A FZD5KI cells, as shown in Figure 2L. The results indicated that Wnt3a or Wnt5a treatment induced the degradation of FZD5 on the cell surface, which was antagonized by cotreatment with RSPO1. We did not perform a more detailed endocytosis/recycling biotinylation experiment that requires complex reversible biotinylation and multiple washing steps because HEK293A cells are fragile in culture and not easy to handle. Furthermore, the results shown in Figure 4 indicate that knockout of ZNRF3/RNF43 or RSPO1 significantly blocked the degradation of internalized FZD5 and reduced the colocalization of internalized FZD5 with lysosomal markers, suggesting that Wnt3a/5a induced lysosomal degradation of FZD5 in the presence of ZNRF3/RNF43 and that the internalized FZD5 was most likely recycled back to the cell surface when ZNRF3/RNF43 was knocked out or inhibited by RSPO1.

> *(2) The authors show that the FZD5 CRD domain is required for endocytosis since a mutant FZD5 protein in which the CRD is removed does not undergo endocytosis. This is perhaps not surprising since this is the site of Wnt binding, but the authors show that a chimeric FZD5CRD-FZD4 receptor can confer Wnt-dependent endocytosis to an otherwise endocytosis incompetent FZD4 protein. Since the linker region between the CRD and the first TM differs between FZD5 and FZD4, it would be interesting to understand whether the CRD specifically or the overall arrangement (such as the spacing) is the most important determinant.*

Our results in Figure 1D-H clearly show that the CRD of FZD5 specifically is both necessary and sufficient for Wnt3a/5a-induced FZD5 endocytosis, as replacing the CRD alone in FZD5 with the CRD from either FZD4 or FZD7 completely abolished Wnt-induced endocytosis, whereas replacing the CRD alone in FZD4 or FZD7 with the FZD5 CRD alone could confer Wnt-induced endocytosis.

> *(3) I find it surprising that only FZD5 and FZD8 appear to undergo endocytosis or be stabilized at the cell surface upon ZNRF3/RNF43 knockout. Is this consistent with previous literature? Is that a cell-specific feature? These findings should be tested in a different cell line, with possibly different relative levels of ZNRF3 and RNF43 expression.*

Thank you for your comments and suggestions. Our finding that ZNRF3/RNF43 specifically regulates FZD5/8 degradation is consistent with recent published studies in which FZD5 is required for the survival of RNF43-mutant PDAC or colorectal cancer cells (Nature Medicine, 2017, PMID: 27869803) and FZD5 is required for the maintenance of intestinal stem cells (Developmental Cell, 2024, PMID: 39579768 and 39579769), and in both cases, FZDs other than FZD5/8 are also expressed but not sufficient to compensate for the function of FZD5. The mechanism by which Wnt3a/5a specifically induces FZD5/8 endocytosis and degradation is currently unknown and needs to be explored in the future. We speculate that Wnt binding to FZD5/8 may recruit another protein on the cell surface to specifically facilitate FZD5/8 endocytosis. On the other hand, we cannot exclude the possibility that Wnts other than Wnt3a/5a may induce the endocytosis and degradation of FZDs other than FZD5/8 since there are 19 Wnts and 10 FZDs in humans. Notably, several previous studies have suggested that ZNRF3/RNF43 may regulate the endocytosis and degradation of all FZDs without selectivity (such as Nature, 2012, PMID: 22575959; Nature, 2012, PMID: 22895187; Mol Cell, 2015, PMID: 25891077). However, their conclusions were drawn mostly on the basis of overexpression studies. According to the results shown in Figure 5E-H, overexpressing a membrane-tethered E3 ligase (such as ZNRF3, RNF43, RNF130, or RNF150) may nonspecifically degrade FZD proteins on the cell surface.

Furthermore, in the revised manuscript, we showed that Wnt3a/5a induced FZD5/8 endocytosis and degradation in multiple cell lines, including Huh7, U2OS, MCF7, and 769P cells (Figure 1-Figure supplement 1 and Figure 2-Figure supplement 1), suggesting that these phenomena are not specific to 293A cells.

> *(4) If FZD7 is not a substrate of ZNRF3/RNF43 and therefore is not ubiquitinated and degraded, how do the authors reconcile that its overexpression does not lead to elevated cytosolic beta-catenin levels in Figure 5B?*

We are currently not sure of the mechanism underlying this result. Considering that most FZDs are expressed in 293A cells, we do not know how much of the mature form of overexpressed FZD7 was presented to the plasma membrane.

> *(5) For Figure 5B, it would be interesting if the authors could evaluate whether overexpression of FZD5 in the ZNRF3/RNF43 double knockout lines would synergize and lead to further increase in cytosolic beta-catenin levels. As control if the substrate selectivity is clear FZD7 overexpression in that line should not do anything.*

Thank you for your suggestion. We performed these experiments as suggested, and the results indicated that overexpressing FZD5 further increased cytosolic beta-catenin levels in ZRDKO cells, whereas FZD7 had no effect (Figure 6D).

> *(6) In Figure 6G, the authors need to show cytosolic levels of beta-catenin in the absence of Wnt in all cases.*

We did not add Wnt CM in this experiment. RSPO1 activity, which relies on endogenous Wnt, has been well documented in previous studies.

> *(7) Since the authors show that DVL is not involved in the Wnt and ZRNF3-dependent endocytosis they should repeat the proximity biotinylation experiment in figure 7 in the DVL triple KO cells. This is an important experiment since previous studies showed that DVL was required for the ZRNF3/RNF43-mediated ubiqtuonation of FZD.*

Thank you for your valuable suggestions. As you suggested, we performed a proximity biotinylation experiment in DVL TKO cells, and the results showed that Wnt3a/5a could still induce the interaction of FZD5 and RNF43 in DVLTKO cells (Figure 7-figure supplement 1), suggesting that the Wnt-induced FZD5−RNF43 interaction is DVL independent.

https://doi.org/10.7554/eLife.103996.2.sa0